An Analytical Model for Solute Transport in Unsaturated Flow through a Single Fracture and Porous Rock Matrix

J. E. Houseworth

Abstract

Exact analytical solutions are presented for solute transport in an unsaturated fracture and porous rock matrix. The problem includes advective transport in the fracture and rock matrix as well as advective and diffusive fracture-matrix exchange. Linear sorption in the fracture and matrix and radioactive decay are also treated. The solution is for steady, uniform transport velocities within the fracture and matrix, but allows for independent specification of each of the velocities. The problem is first solved in terms of the solute concentrations that result from an instantaneous point source. Superposition integrals are then used to derive the solute mass flux at a fixed downstream position from an instantaneous point source and for the solute concentrations that result from a continuous point source. Solutions are derived for cases with the solute source in the fracture and the solute source in the matrix. The analytical solutions are closed-form and are expressed in terms of algebraic functions, exponentials, and error functions. Comparisons between the analytical solutions and numerical simulations, as well as sensitivity studies, are presented. Increased sensitivity to cross-flow and solute source location is found for increasing Peclet number. The numerical solutions are found to compare well with the analytical solutions at lower Peclet numbers, but show greater deviation at higher Peclet numbers.

1. Introduction

Transport in fractured rock typically results from a combination of relatively fast transport in fractures coupled with much slower transport in the rock matrix. Fracture pathways typically carry most of the flow but have relatively small water content; therefore transport velocities in fractures are high. The rock matrix lying between fractures often carries a smaller fraction of the total flow, but is dominant in terms of bulk water content, leading to much lower transport velocities. Transport through saturated fractured rock was investigated in analytical models by Tang et al. (1981) and Sudicky and Frind (1982). Although complete water saturation is not a strict requirement for the application of these models, they are limited to diffusive exchange between fractures and matrix, with no flow in the matrix.

Advection through the rock matrix can affect transport of solutes in fractured rock. Flow in the rock matrix results from both capillary and gravity forces. In unsaturated fractured rock systems, advective transport between the fractures and matrix may occur as a result of flow driven by differences in capillary pressure. Such effects have been noted to result in slower transport because capillary pressure conditions typically lead to flow from the fractures to the matrix (Ho, 2001). On the other hand, advection through the matrix in the direction of the mean flow will facilitate overall transport. Therefore, the effects of advection in the matrix on solute transport can affect transport in qualitatively different ways.

An analytical model for transport in a single fracture through a porous rock matrix is presented here. This model includes three independent advective velocities for global fracture and matrix advective transport and advective fracture-matrix exchange. The

model also treats diffusive exchange between the fractures and matrix, linear sorption in the fracture and matrix, and radioactive decay.

The problems to be solved are shown in Figures 1a and 1b. These figures represent solute transport in a single fracture through a porous rock matrix with the initial solute source in the fracture (Figure 1a) or matrix (Figure 1b). The analyses presented here are restricted to the following conditions:

1. Steady, spatially uniform flow in parallel plane fracture and associate rock matrix.
2. Two-dimensional geometry, semi-infinite domain longitudinally and infinite domain laterally.
3. Longitudinal diffusion and dispersion are negligible.
4. Advective transport velocity in the fracture is larger than the advective transport velocity in the matrix.
5. Transverse mixing in the fracture produces a uniform concentration across the fracture-water film.

Condition 1 is needed to restrict the flow sufficiently for analytical treatment of the transport problem. This restricts the class of problems to those in which the cross-flow is a small in comparison to the flow through the fracture and rock matrix. Such conditions are expected when capillary pressure differences between the fracture and matrix water are small. Cross-flow between the fracture and rock matrix is idealized as flow driven by a uniform capillary pressure gradient laterally across the matrix. Condition 2 concerning the problem's geometry is also needed to specify and simplify the problem for analytical treatment. Longitudinal dispersion is neglected, as stated in condition 3, to simplify the problem but in actual applications involving dual-permeability systems this is generally a good approximation. Fracture-matrix exchange, which is included explicitly, will typically predominate over other longitudinal diffusive or dispersive processes. This restriction is investigated further in Section 5.5. Condition 4 is generally true if fracture flow is a significant factor in the system. Condition 5 is also generally true because diffusion is effective at lateral mixing across the thin water films typical of flow in fractures.

Transport occurs in the longitudinal direction due to advection. The initial condition for the matrix solute source is symmetric about the fracture centerline, i.e., one point source on each side of each fracture at equal distances from fracture-matrix interface. Independent and distinct longitudinal velocities are allowed for the fracture and matrix, subject to condition 4. Exchange between the fracture and matrix occur through both advection and diffusion. Although flow between these domains is expected to be primarily from the fracture to the matrix because of the typically higher capillary pressures in the matrix as compared to the fractures, the model is also applicable to advective exchange in either direction. Independent and distinct linear sorption is included in the formulation for the fracture and the matrix, leading to retardation factors for each domain.

Coupled transport equations for solute transport through the fracture and the rock matrix are developed in Section 2. The coupling takes the form of a distributed source term in the conservation equation for the fracture and a boundary condition for the rock matrix. The two-dimensional transport problem in the rock matrix is reduced to a one-dimensional problem through a transformation to a coordinate system that moves at the longitudinal advective velocity in the rock matrix. The equations and boundary conditions are then transformed into dimensionless form. The solution for the solute concentration from an instantaneous point source in the fracture is presented in Sections 3.1 and 3.2 using a Laplace transform method. Integrated forms of the solution representing the cumulative mass arrivals at a downstream location and concentrations from a continuous source are derived in Sections 3.3 and 3.4, respectively. Analogous solutions for a point source in the rock matrix are presented in Section 4. Comparisons with numerical simulations and sensitivity analyses are presented in Section 5.

2. Mathematical Formulation

2.1 Development of Conservation Equations

The conservation equation for solute mass transport in a fracture is,

$$\phi_f S_f \left(\frac{\partial c_f}{\partial t} + \lambda c_f \right) + \rho_{bf} \left(\frac{\partial c_{fa}}{\partial t} + \lambda c_{fa} \right) + q_f \frac{\partial c_f}{\partial z} = A_{vfm} A_r \left(\phi_m S_m D_m \left. \frac{\partial c_m}{\partial x} \right|_{x=0} - q_{fm} c_m \big|_{x=0} \right) \quad (1)$$

The first two terms on the left-hand side of Equation (1) represent the rate of change in solute mass as a dissolved and sorbed species, respectively, including radioactive decay (see Notation at the end of the paper for a definition of mathematical terms). The third term represents the gradient in the advective solute mass flux through the fracture. The two terms on the right hand side of Equation (1) represent the diffusive and advective exchange of solute mass between the fracture and the rock matrix. Note that the fracture porosity allows for rock mass within the fracture volume that may participate in reactions with the solute resulting in sorption during transport through the fracture.

For a plane-parallel fracture, the fracture-matrix interface area for some representative fracture control volume is two times the fracture length (z-direction) times the fracture depth (y-direction). The fracture bulk volume for this same control volume is the fracture aperture, b, times the same length and depth. Therefore, the fracture-matrix interface area per unit fracture volume is,

$$A_{vfm} = \frac{2}{b} \quad (2)$$

The fracture-matrix interface area per unit volume is multiplied by an area reduction factor, A_r. This factor is introduced to acknowledge the possibility that the fracture water contact with the rock matrix may be less than the full geometric contact area represented in Equation (2). Such a reduction factor has been postulated for unsaturated

flow to account for effects such as flow instability, heterogeneity, and preferential flow (Liu et al., 1998; Doughty 1999).

Similarly, the fracture water flux, q_f, is given by the volumetric flow rate per unit fracture depth (*y*-direction) through the representative fracture volume, Q_f, divided by the fracture aperture,

$$q_f = \frac{Q_f}{b} \tag{3}$$

For a linear sorption process,

$$c_{fa} = K_{df} c_f \tag{4}$$

where K_{df} is the linear sorption coefficient in units of solution volume per unit rock mass.

Using Equations (2) through (4) in Equation (1) gives,

$$\frac{\partial c_{f\lambda}}{\partial t} + v_f \frac{\partial c_{f\lambda}}{\partial z} = \left(\frac{2A_r}{b}\right)\left(\frac{\phi_m S_m R_m}{\phi_f S_f R_f}\right)\left(D_m^* \frac{\partial c_{m\lambda}}{\partial x}\bigg|_{x=0} - v_{fm} c_{m\lambda}\big|_{x=0}\right) \tag{5}$$

where

$R_f = 1 + \dfrac{\rho_{bf} K_{df}}{\phi_f S_f}$ is the retardation coefficient in for transport in the fractures

$v_f = \dfrac{Q_f}{b\phi_f S_f R_f}$ is the advective transport velocity in the fractures.

$v_{fm} = \dfrac{q_{fm}}{\phi_m S_m R_m}$ is the advective transport velocity in the matrix (*x*-direction)

$D_m^* = \dfrac{D_m}{R_m}$ and R_m is the retardation factor for transport in the matrix (defined below)

and $c_{f\lambda}$ and $c_{m\lambda}$ are the solute mass concentrations in the fracture and matrix waters, respectively, multiplied by the radioactive decay factor, $e^{\lambda t}$.

The conservation equation for solute mass transport in the rock matrix is,

$$\phi_m S_m \left(\frac{\partial c_m}{\partial t} + \lambda c_m\right) + \rho_{bm}\left(\frac{\partial c_{ma}}{\partial t} + \lambda c_{ma}\right) + q_m \frac{\partial c_m}{\partial z} + q_{fm} \frac{\partial c_m}{\partial x} = \phi_m S_m D_m \frac{\partial^2 c_m}{\partial x^2} \tag{6}$$

The first two terms on the left-hand side of Equation (8) represent the rate of change in solute mass as a dissolved and sorbed species, respectively, including radioactive decay. The third and fourth terms represent the gradient in the advective solute mass flux through the matrix in the longitudinal and transverse directions, respectively. The term on the right hand side of Equation (8) represents the gradient in the transverse diffusive flux through the rock matrix.

For a linear sorption process,

$$c_{ma} = K_{dm} c_m \tag{7}$$

where K_{dm} is the linear sorption coefficient in the rock matrix.

Using Equation (7) in Equation (6) gives,

$$\frac{\partial c_{m\lambda}}{\partial t} + v_m \frac{\partial c_{m\lambda}}{\partial z} + v_{fm} \frac{\partial c_{m\lambda}}{\partial x} = D_m^* \frac{\partial^2 c_{m\lambda}}{\partial x^2} \tag{8}$$

where

$R_m = 1 + \dfrac{\rho_{bm} K_{dm}}{\phi_m S_m}$ is the retardation coefficient for transport in the matrix.

$v_m = \dfrac{q_m}{\phi_m S_m R_m}$ is the advective transport velocity in the matrix in the *z* direction.

2.2 Boundary Conditions

The boundary condition in fracture is,

$$\lim_{z \to -\infty} c_{f\lambda}(z,t) = 0 \tag{9}$$

This is a result of the fact that no tracer can exist for $z < v_m t$, provided an initial source at $z = 0$.

The boundary condition for solute transport in the rock matrix at the fracture interface is that the solute concentrations in the fracture and matrix are equal,

$$c_{m\lambda}(0,z,t) = c_{f\lambda}(z,t) \tag{10}$$

Given a semi-infinite domain for the rock matrix, the solute concentration as $x \to \infty$ is zero,

$$\lim_{x \to \infty} c_{m\lambda}(x,z,t) = 0 \tag{11}$$

2.3 Initial Condition – Fracture Solute Source

The initial condition in the fracture is an instantaneous point source represented as a delta function,

$$c_{f\lambda}(z,0) = \frac{M_0}{A_f \phi_f S_f R_f}\,\delta(z) \tag{12}$$

where A_f is the fracture cross-sectional area orthogonal to the z axis, M_0 is the initial mass of solute (including solute sorbed), and $\delta(z)$ is the delta function.

This initial condition is defined to ensure the following total solute mass condition,

$$A_f \phi_f S_f R_f \int_{-\infty}^{\infty} c_{f\lambda}(z,0)\,dz = M_0 \tag{13}$$

The initial condition for solute mass in the rock matrix is zero concentration given the initial solute source in the fracture,

$$c_{m\lambda}(x,z,0) = 0 \tag{14}$$

The initial condition for a matrix solute source is given in Section 4.1.

2.4 Transformation to a Moving Coordinate System

Introduce a transformation to moving coordinate system. Let

$$\varsigma = z - v_m t \tag{15}$$

Using Equation (15), Equations (5) becomes,

$$\frac{\partial c_{f\lambda}}{\partial t} + v_f^* \frac{\partial c_{f\lambda}}{\partial \varsigma} = \left(\frac{2A_r}{b}\right)\left(\frac{\phi_m S_m R_m}{\phi_f S_f R_f}\right)\left(D_m^* \frac{\partial c_{m\lambda}}{\partial x}\bigg|_{x=0} - v_{fm}\, c_{m\lambda}\big|_{x=0}\right) \tag{16}$$

where $v_f^* = v_f - v_m$ is the longitudinal velocity in the fracture relative to the matrix.

The boundary and initial conditions, Equations (9) and (12), for the fracture become, respectively,

$$\lim_{\varsigma \to -\infty} c_{f\lambda}(\varsigma,t) = 0 \tag{17}$$

$$c_{f\lambda}(\varsigma,0) = \frac{M_0}{A_f \phi_f S_f R_f}\,\delta(\varsigma) \tag{18}$$

The conservation equation for the matrix, Equation (8) under this transformation becomes,

$$\frac{\partial c_{m\lambda}}{\partial t} + v_{fm}\frac{\partial c_{m\lambda}}{\partial x} = D_m^* \frac{\partial^2 c_{m\lambda}}{\partial x^2} \tag{19}$$

Note that the multidimensional advective transport in the matrix as expressed in Equation (8) is now reduced to a single dimension in the transverse direction. The boundary and initial conditions for the matrix as given in Equations (10), (11), and (14) become, respectively,

$$c_{m\lambda}(0,\varsigma,t) = c_{f\lambda}(\varsigma,t) \tag{20}$$

$$\lim_{x \to \infty} c_{m\lambda}(x,\varsigma,t) = 0 \tag{21}$$

$$c_{m\lambda}(x,\varsigma,0) = 0 \tag{22}$$

2.5 Transformation to Dimensionless Form

The collection of terms found on the right-hand side of Equation (16) is a convenient length scale, ℓ, for the development of nondimensional variables,

$$\ell = \frac{b}{2A_r}\frac{\phi_f S_f R_f}{\phi_m S_m R_m} \tag{23}$$

Note that this length scale represents an effective fracture water volume divided by the corresponding effective matrix water area in contact with the fracture water (see also Equation (2)). The length scale also accounts for the effects of sorption through the retardation factors, which represent additional solute storage resulting from sorption.

With this length scale, the following dimensionless variables may be defined:

$$\tau = \frac{v_f^* t}{\ell} \tag{24}$$

$$\xi = \frac{\varsigma}{\ell} \tag{25}$$

$$\eta = \frac{x}{\ell} \tag{26}$$

$$c_{fd} = \frac{A_f \phi_f S_f R_f \ell}{M_0} c_{f\lambda} \tag{27}$$

$$c_{md} = \frac{A_f \phi_f S_f R_f \ell}{M_0} c_{m\lambda} \tag{28}$$

Using these dimensionless variables, Equation (16) becomes

$$\frac{\partial c_{fd}}{\partial \tau} + \frac{\partial c_{fd}}{\partial \xi} = \frac{1}{Pe} \frac{\partial c_{md}}{\partial \eta}\bigg|_{\eta=0} - V c_{md}\big|_{\eta=0} \tag{29}$$

where

$$Pe = \frac{v_f^* \ell}{D_m^*} \tag{30}$$

is the Peclet number and

$$V = \frac{v_{fm}}{v_f^*} \tag{31}$$

is the cross-flow velocity ratio. The boundary and initial conditions for the fracture, Equations (17) and (18), respectively, become,

$$\lim_{\xi \to -\infty} c_{fd}(\xi, \tau) = 0 \tag{32}$$

$$c_{fd}(\xi, 0) = \delta(\xi) \tag{33}$$

Note that the nondimensional delta function in Equation (33) is related to the delta function in Equation (17) through the following total mass condition at $t = 0$,

$$\int_{-\infty}^{\infty} \delta(\xi) d\xi = \int_{-\infty}^{\infty} \frac{1}{\ell} \delta(\xi) dz = \int_{-\infty}^{\infty} \delta(z) dz \quad \therefore \delta(\xi) = \ell \delta(z)$$

Using the nondimensional variables, Equation (19) becomes,

$$\frac{\partial c_{md}}{\partial \tau} + V \frac{\partial c_{md}}{\partial \eta} = \frac{1}{Pe} \frac{\partial^2 c_{md}}{\partial \eta^2} \tag{34}$$

The nondimensional forms for the boundary and conditions in Equations (20), (21), and (22) are, respectively,

$$c_{md}(0,\xi,\tau) = c_{fd}(\xi,\tau) \tag{35}$$

$$\lim_{\eta \to \infty} c_{md}(\eta,\xi,\tau) = 0 \tag{36}$$

$$c_{md}(\eta,\xi,0) = 0 \tag{37}$$

3. Mathematical Solution – Fracture Solute Source

3.1 Solution for the Laplace Transformed Matrix and Fracture Concentrations

The Laplace transform may be represented as the following integral change of variables,

$$H(\tau)c_{md}(\eta,\xi,\tau) = \frac{1}{2\pi i}\int_{c-i\infty}^{c+i\infty} \hat{c}_{md}(\eta,\xi,s)e^{s\tau}\, ds \tag{38}$$

$$H(\tau)c_{fd}(\xi,\tau) = \frac{1}{2\pi i}\int_{c-i\infty}^{c+i\infty} \hat{c}_{fd}(\xi,s)e^{s\tau}\, ds \tag{39}$$

where $H(\tau)$ is the step function defined by,

$H(\tau) = 0;\ \tau \le 0$
$H(\tau) = 1;\ \tau > 0$

Substituting Equation (38) for c_{md} in Equation (34) leads to the following differential equation in terms of $\hat{c}_{md}$,

$$\frac{d^2\hat{c}_{md}}{d\eta^2} - Pe\,V\frac{d\,\hat{c}_{md}}{d\eta} - s\,Pe\hat{c}_{md} = 0 \tag{40}$$

The solution to Equation (40) that is consistent with the transformed initial and boundary conditions from Equations (35) and (36) is,

$$\hat{c}_{md}(\eta,\xi,s) = \hat{c}_{fd}(\xi,s)\exp\left[\left(\frac{PeV}{2} - \sqrt{\left(\frac{PeV}{2}\right)^2 + s\,Pe}\right)\eta\right] \tag{41}$$

The fracture solute mass conservation equation, given in Equation (29), becomes the following using Equations (38) and (39) subject to the initial condition in Equation (33),

$$\frac{\partial \hat{c}_{fd}}{\partial \xi} + s\,\hat{c}_{fd} - \frac{1}{Pe}\frac{\partial \hat{c}_{md}}{\partial \eta}\bigg|_{\eta=0} + V\,\hat{c}_{md}\big|_{\eta=0} = \delta(\xi) \tag{42}$$

Substituting Equation (41) for $\hat{c}_{md}$ into Equation (42) gives,

$$\frac{d\hat{c}_{fd}}{d\xi} + \left\{ s + \frac{V}{2} + \sqrt{\frac{V^2}{4} + \frac{s}{Pe}} \right\} \hat{c}_{fd} = \delta(\xi) \tag{43}$$

Integrating Equation (43) from $-\infty$ to ξ and using Equation (32) gives,

$$\hat{c}_{fd}(\xi, s) = \exp\left[-\left(s + \frac{V}{2} + \sqrt{\frac{V^2}{4} + \frac{s}{Pe}} \right) \xi \right] H(\xi) \tag{44}$$

where $H(\xi)$ is the step function.

3.2 Inversion of the Laplace Transformed Solutions

The convolution theorem is used to simplify the dependence on *s* in Equation (44). The convolution theorem states,

$$\int_0^{\tau} F_1(\tau - \sigma) F_2(\sigma)\, d\sigma = \frac{1}{2\pi i} \int_{c-i\infty}^{c+i\infty} f_1(s) f_2(s) e^{s\tau}\, ds \tag{45}$$

Let

$$f_1(s) = e^{-s\xi} \tag{46}$$

which implies

$$F_1(\tau) = \delta(\tau - \xi) \tag{47}$$

and let

$$f_2(s) = \exp\left[-\left(\frac{V}{2} + \sqrt{\frac{V^2}{4} + \frac{s}{Pe}} \right) \xi \right] H(\xi) \tag{48}$$

so that

$$F_2(\tau) = \frac{1}{2\pi i}\int_{c-i\infty}^{c+i\infty} H(\xi)\exp\left[-\left(\frac{V}{2}+\frac{1}{\sqrt{Pe}}\sqrt{\frac{PeV^2}{4}+s}\right)\xi + s\tau\right] ds \tag{49}$$

To evaluate F_2, let

$$\chi = s + \frac{PeV^2}{4} \tag{50}$$

Substituting Equation (50) into (49) gives

$$F_2(\tau) = H(\xi)\exp\left[-\frac{V\xi}{2}-\frac{PeV^2\tau}{4}\right]\frac{1}{2\pi i}\int_{c+\frac{PeV^2}{4}-i\infty}^{c+\frac{PeV^2}{4}+i\infty} \exp\left[-\frac{\xi\sqrt{\chi}}{\sqrt{Pe}}+\chi\tau\right] d\chi \tag{51}$$

which is tabulated to give (Abramowitz and Stegun, 1972, Equation 29.3.82),

$$F_2(\tau) = H(\xi)\exp\left[-\frac{V\xi}{2}-\frac{PeV^2\tau}{4}\right]\left(\frac{\xi}{2\sqrt{\pi}\sqrt{Pe}\tau^{3/2}}\right)\exp\left[\frac{-\xi^2}{4Pe\tau}\right] \tag{52}$$

Integrating Equation (45) using Equations (47) and (52) and using the definition of $\hat{c}_{fd}$ in Equation (39) and integrating gives,

$$c_{fd}(\xi,\tau) = H(\xi)H(\tau-\xi)\left(\frac{\xi}{2\sqrt{\pi}\sqrt{Pe}(\tau-\xi)^{3/2}}\right)\exp\left[-\left\{\frac{\xi+PeV(\tau-\xi)}{2\sqrt{Pe}\sqrt{\tau-\xi}}\right\}^2\right] \tag{53}$$

The dimensionless fracture concentration is a function of the dimensionless longitudinal position, dimensionless time, Peclet number and cross-flow velocity ratio. To obtain the solution for the matrix concentration, substitute Equation (44) into Equation (41) to give,

$$\hat{c}_{md}(\eta,\xi,s) = H(\xi)\exp\left[-\left(s+\frac{V}{2}+\sqrt{\frac{V^2}{4}+\frac{s}{Pe}}\right)\xi\right]\exp\left[\left(\frac{PeV}{2}-\sqrt{\left(\frac{PeV}{2}\right)^2+s\,Pe}\right)\eta\right] \tag{54}$$

which upon rearranging, gives

$$\hat{c}_{md}(\eta,\xi,s) = H(\xi)\exp\left[-\frac{V}{2}(\xi-Pe\eta)\right]\exp(-s\xi)\exp\left[-\left(\frac{\xi}{\sqrt{Pe}}+\sqrt{Pe}\eta\right)\sqrt{\frac{PeV^2}{4}+s}\right] \tag{55}$$

Following a similar series of steps as performed for the inversion of the fracture concentration using the convolution theorem, the solution for the matrix concentration is found to be,

$$c_{md}(\eta,\xi,\tau) = H(\xi)H(\tau-\xi)\exp[-\xi V]\frac{(\xi+Pe\eta)}{2\sqrt{\pi}\sqrt{Pe}(\tau-\xi)^{3/2}}\exp\left[-\left\{\frac{Pe\eta+\xi-Pe\,V(\tau-\xi)}{2\sqrt{Pe}\sqrt{\tau-\xi}}\right\}^2\right] \quad (56)$$

The dimensionless matrix concentration is a function of the dimensionless transverse position in addition to the other factors that were found to affect the dimensionless fracture concentration. Equations (53) and (56) are the complete solution for the solute concentration resulting from an instantaneous point source located in the fracture.

3.3 Cumulative Mass Arrivals at a Downstream Location

The description of transport from a given source is often represented as a breakthrough curve, which gives the cumulative mass arrival relative to the total mass release at some point downstream of the source. Mathematically, this is the time integral of the mass flux at the downstream location divided by the total source mass.

For the fracture, the integrated mass flux over time at a fixed downstream position, $z_{0,}$ is,

$$M_f(T) = \int_0^T A_f\phi_f S_f R_f v_f c_f(z_0,t)dt \quad (57)$$

where T is the time of observation. Using the definition of the dimensionless concentration in Equation (27), the cumulative flux integral becomes,

$$\frac{M_f}{M_0}(T) = \int_0^T c_{fd}(z_0,t)\exp\left\{-\left(\frac{\lambda\ell}{v_f}\right)\left(\frac{v_f t}{\ell}\right)\right\}d\left(\frac{v_f t}{\ell}\right) \quad (58)$$

Define the following dimensionless variables,

$$\sigma = \frac{v_f t}{\ell} \quad (59)$$

$$\psi = \frac{v_f T}{\ell} \quad (60)$$

and

$$\lambda_d = \frac{\lambda\ell}{v_f} \quad (61)$$

Also, using the definition of ξ (see Equations (15) and (25)), define the following variables:

$$\xi_0 = \zeta_0 - V_\ell\sigma \quad (62)$$

such that $\tau - \xi_0 = \sigma - \zeta_0$ where

$$\zeta_0 = \frac{z_0}{\ell} \tag{63}$$

is the dimensionless flux boundary position and

$$V_\ell = \frac{v_m}{v_f} \tag{64}$$

is the longitudinal velocity ratio.

Using Equations (59), (60), (61), and (63)in Equation (58) gives

$$\frac{M_f}{M_0}(\psi) = \int_0^{\psi} c_{fd}(\zeta_0, \sigma)\exp(-\lambda_d \sigma)d\sigma \tag{65}$$

The details of the integration of Equation (65) using Equation (53) for c_{fd} are given in Appendix I. The result is,

$$\begin{aligned}\frac{M_f}{M_0}(\psi) = {} & \frac{\exp\left[-\frac{\zeta_0}{2Pe}\left\{(1-V_\ell)(PeV-V_\ell)+2Pe\lambda_d\right\}\right]}{2\left\{(PeV-V_\ell)^2+4Pe\lambda_d\right\}^{\frac{1}{2}}} \bullet \\ & \left[\begin{array}{l} \left\{\left\{(PeV-V_\ell)^2+4Pe\lambda_d\right\}^{\frac{1}{2}}+V_\ell\right\}\exp\left[\frac{\zeta_0(1-V_\ell)}{2Pe}\left\{(PeV-V_\ell)^2+4Pe\lambda_d\right\}^{\frac{1}{2}}\right]\bullet \\ \quad \operatorname{erfc}\left\{\frac{\left\{(PeV-V_\ell)^2+4Pe\lambda_d\right\}^{\frac{1}{2}}(\psi-\zeta_0)+\zeta_0(1-V_\ell)}{2\sqrt{Pe}\sqrt{\psi-\zeta_0}}\right\} \\ -\left\{\left\{(PeV-V_\ell)^2+4Pe\lambda_d\right\}^{\frac{1}{2}}-V_\ell\right\}\exp\left[-\frac{\zeta_0(1-V_\ell)}{2Pe}\left\{(PeV-V_\ell)^2+4Pe\lambda_d\right\}^{\frac{1}{2}}\right]\bullet \\ \quad \operatorname{erfc}\left\{\frac{\left\{(PeV-V_\ell)^2+4Pe\lambda_d\right\}^{\frac{1}{2}}(\psi-\zeta_0)-\zeta_0(1-V_\ell)}{2\sqrt{Pe}\sqrt{\psi-\zeta_0}}\right\} \end{array}\right] \end{aligned} \tag{66}$$

for $\zeta_0 \le \psi \le \frac{\zeta_0}{V_\ell}$. For $\psi < \zeta_0$, $\frac{M_f}{M_0}(\psi) = 0$ and for $\psi > \frac{\zeta_0}{V_\ell}$, $\frac{M_f}{M_0}(\psi) = \frac{M_f}{M_0}\left(\frac{\zeta_0}{V_\ell}\right)$.

The relative cumulative mass is found to be a function of the dimensionless observation time, and also depends on the dimensionless downstream position, Peclet number, cross-flow velocity ratio, and longitudinal velocity ratio. The bounds on the solution between

ζ_0 and $\frac{\zeta_0}{V_\ell}$ represent the fastest and slowest possible travel times to the downstream boundary defined by the downstream distance divided by the fracture and matrix longitudinal velocities, respectively.

For the matrix, we also integrate the mass flux over time at a fixed position, z_0. However, in this case, the integration is also performed over the cross-sectional direction, x, as given by,

$$M_m(T) = 2\int_0^T \left(\frac{A_f A_r}{b} \right) \phi_m S_m R_m v_m \int_0^\infty c_m(x, z_0, t)\, dx\, dt \tag{67}$$

Note that the 2 is needed to account for tracer mass on both sides of each fracture. The term $\frac{A_f A_r}{b}$ is the depth dimension.

Using Equation (28) in Equation (67) gives

$$\frac{M_m}{M_0}(T) = \frac{2A_r}{b\ell} \frac{\phi_m S_m R_m}{\phi_f S_f R_f} \frac{v_m}{v_f} \ell^2 \int_0^T \int_0^\infty c_{md}(x, z, t) \exp\left\{ -\left(\frac{\lambda \ell}{v_f} \right) \left(\frac{v_f t}{\ell} \right) \right\} d\left(\frac{x}{\ell} \right) d\left(\frac{v_f t}{\ell} \right) \tag{68}$$

Noting the definition of ℓ in Equation (23) and the previously defined dimensionless variables gives for Equation (67),

$$\frac{M_m}{M_0}(\psi) = V_\ell \int_0^\psi \int_0^\infty c_{md}(\eta, \zeta_0, \sigma) \exp(-\lambda_d \sigma)\, d\eta\, d\sigma \tag{69}$$

The integration of Equation (69) using Equation (56) for c_{md} is similar to that shown in Appendix I for the derivation of Equation (66). The result is,

$$\frac{M_m}{M_0}(\psi) = \frac{-V_\ell \exp\left\{-\frac{\zeta_0}{2Pe}\left[(1-V_\ell)(PeV-V_\ell)+2Pe\lambda_d\right]\right\}}{4(VV_\ell-\lambda_d)\left\{(PeV-V_\ell)^2+4Pe\lambda_d\right\}^{\frac{1}{2}}} \bullet$$

$$\left[\begin{array}{l}
\left(4(VV_\ell-\lambda_d)-V\left[PeV+V_\ell-\left\{(PeV-V_\ell)^2+4Pe\lambda_d\right\}^{\frac{1}{2}}\right]\right)\bullet \\
\exp\left(\frac{\zeta_0(1-V_\ell)}{2Pe}\left\{(PeV-V_\ell)^2+4Pe\lambda_d\right\}^{\frac{1}{2}}\right)\bullet \\
\operatorname{erfc}\left(\frac{\left\{(PeV-V_\ell)^2+4Pe\lambda_d\right\}^{\frac{1}{2}}(\psi-\zeta_0)+\zeta_0(1-V_\ell)}{2\sqrt{Pe}\sqrt{\psi-\zeta_0}}\right) \\
+\left(4(VV_\ell-\lambda_d)-V\left[PeV+V_\ell+\left\{(PeV-V_\ell)^2+4Pe\lambda_d\right\}^{\frac{1}{2}}\right]\right)\bullet \\
\exp\left(-\frac{\zeta_0(1-V_\ell)}{2Pe}\left\{(PeV-V_\ell)^2+4Pe\lambda_d\right\}^{\frac{1}{2}}\right)\bullet \\
\operatorname{erfc}\left(\frac{\left\{(PeV-V_\ell)^2+4Pe\lambda_d\right\}^{\frac{1}{2}}(\psi-\zeta_0)-\zeta_0(1-V_\ell)}{2\sqrt{Pe}\sqrt{\psi-\zeta_0}}\right)
\end{array}\right] \qquad (70)$$

$$-\frac{VV_\ell}{2(VV_\ell-\lambda_d)}\exp\left\{-V\zeta_0\left(1-V_\ell+\frac{\lambda_d}{V}\right)\right\}\exp\left[(VV_\ell-\lambda_d)(\psi-\zeta_0)\right]\bullet$$

$$\operatorname{erfc}\left\{\frac{(PeV+V_\ell)(\psi-\zeta_0)-\zeta_0(1-V_\ell)}{2\sqrt{Pe}\sqrt{\psi-\zeta_0}}\right\}$$

for $\zeta_0 \le \psi \le \frac{\zeta_0}{V_\ell}$. For $\psi < \zeta_0$, $\frac{M_m}{M_0}(\psi) = 0$ and for $\psi > \frac{\zeta_0}{V_\ell}$, $\frac{M_m}{M_0}(\psi) = \frac{M_m}{M_0}\left(\frac{\zeta_0}{V_\ell}\right)$.

The combined cumulative mass arrival at the downstream location is given by the sum of Equations (66) and (70).

$$\frac{M_f + M_m}{M_0}(\psi) = \frac{\exp\left\{-\frac{\zeta_0}{2Pe}\left[(1-V_\ell)(PeV - V_\ell) + 2Pe\lambda_d\right]\right\}}{4(VV_\ell - \lambda_d)\left\{(PeV - V_\ell)^2 + 4Pe\lambda_d\right\}^{\frac{1}{2}}} \bullet$$

$$\left[\begin{array}{l}
\left\{VV_\ell\left[PeV - \left(1 - \frac{2\lambda_d}{VV_\ell}\right)\left(V_\ell - \left\{(PeV - V_\ell)^2 + 4Pe\lambda_d\right\}^{\frac{1}{2}}\right)\right]\right\} \bullet \\
\exp\left(\frac{\zeta_0(1-V_\ell)}{2Pe}\left\{(PeV - V_\ell)^2 + 4Pe\lambda_d\right\}^{\frac{1}{2}}\right) \bullet \\
\operatorname{erfc}\left(\frac{\left\{(PeV - V_\ell)^2 + 4Pe\lambda_d\right\}^{\frac{1}{2}}(\psi - \zeta_0) + \zeta_0(1-V_\ell)}{2\sqrt{Pe}\sqrt{\psi - \zeta_0}}\right) \\
+\left\{VV_\ell\left[PeV - \left(1 - \frac{2\lambda_d}{VV_\ell}\right)\left(V_\ell + \left\{(PeV - V_\ell)^2 + 4Pe\lambda_d\right\}^{\frac{1}{2}}\right)\right]\right\} \bullet \\
\exp\left(-\frac{\zeta_0(1-V_\ell)}{2Pe}\left\{(PeV - V_\ell)^2 + 4Pe\lambda_d\right\}^{\frac{1}{2}}\right) \bullet \\
\operatorname{erfc}\left(\frac{\left\{(PeV - V_\ell)^2 + 4Pe\lambda_d\right\}^{\frac{1}{2}}(\psi - \zeta_0) - \zeta_0(1-V_\ell)}{2\sqrt{Pe}\sqrt{\psi - \zeta_0}}\right)
\end{array}\right]$$

$$-\frac{VV_\ell}{2(VV_\ell - \lambda_d)}\exp\left\{-V\zeta_0\left(1 - V_\ell + \frac{\lambda_d}{V}\right)\right\}\exp\left[(VV_\ell - \lambda_d)(\psi - \zeta_0)\right] \bullet$$

$$\operatorname{erfc}\left\{\frac{(PeV + V_\ell)(\psi - \zeta_0) - \zeta_0(1-V_\ell)}{2\sqrt{Pe}\sqrt{\psi - \zeta_0}}\right\} \qquad (71)$$

for $\zeta_0 \le \psi \le \frac{\zeta_0}{V_\ell}$. For $\psi < \zeta_0$, $\frac{M_f + M_m}{M_0}(\psi) = 0$ and for $\psi > \frac{\zeta_0}{V_\ell}$,

$\frac{M_f + M_m}{M_0}(\psi) = \frac{M_f + M_m}{M_0}\left(\frac{\zeta_0}{V_\ell}\right)$.

For a non-decaying solute ($\lambda = 0$), the result in Equation (71) simplifies to,

$$\frac{M_f + M_m}{M_0}(\psi) = \frac{1}{2}\operatorname{erfc}\left\{\frac{\zeta_0 - V_\ell\psi + PeV(\psi - \zeta_0)}{2\sqrt{Pe}\sqrt{\psi - \zeta_0}}\right\}$$

$$+\frac{1}{2}\exp\left\{-V\left(\zeta_0 - V_\ell\psi\right)\right\}\operatorname{erfc}\left\{\frac{\zeta_0 - V_\ell\psi - PeV(\psi - \zeta_0)}{2\sqrt{Pe}\sqrt{\psi - \zeta_0}}\right\} \qquad (72)$$

3.4 Concentration from a Continuous Point Source

The concentration field that evolves from a continuous point source, c_{fcs}, may be derived through superposition in time of the solution for an instantaneous point source,

$$c_{fcs}(z,T) = \int_0^T \frac{1}{M_0}\frac{\partial M}{\partial \tau} c_f(z, T-\tau)\, d\tau \tag{73}$$

where c_f is the concentration from an instantaneous release in the fracture based on a mass M_0, and c_{fcs} is the resulting concentration from a continuous solute mass source released at a constant rate of $\frac{\partial M}{\partial \tau} = \dot{M}$. Note in what follows that T is the time of observation and τ represents the time of source release.

Equation (73) may be transformed to dimensionless form using Equation (27),

$$c_{fcs}(\zeta,\psi) = \frac{\dot{M}}{A_f \phi_f S_f R_f v_f} \int_0^{\psi} c_{fd}(\zeta, \psi-\sigma)\exp\{-\lambda_d(\psi-\sigma)\}\, d\sigma \tag{74}$$

where as before,

$$\psi = \frac{v_f T}{\ell}\ ,\ \sigma = \frac{v_f \tau}{\ell},\ \zeta = \frac{z}{\ell}$$

and

$$\lambda_d = \frac{\lambda \ell}{v_f}$$

Let

$$c_{fcsd} = \frac{A_f \phi_f S_f R_f v_f}{\dot{M}} c_{fcs} \tag{75}$$

Substituting Equation (75) into (74) gives,

$$c_{fcsd}(\zeta,\psi) = \int_0^{\psi} c_{fd}(\zeta, \psi-\sigma)\exp\{-\lambda_d(\psi-\sigma)\}\, d\sigma \tag{76}$$

Let $\mu = \psi - \sigma$. Then $d\mu = -d\sigma$; $\mu = \psi$ at $\sigma = 0$; $\mu = 0$ at $\sigma = \psi$

Then,

$$c_{fcsd}(\zeta,\psi)=\int_0^{\psi} c_{fd}(\zeta,\mu)\exp(-\lambda_d\mu)d\mu \tag{77}$$

This integral is the same as evaluated for the mass flux at a fixed position in Equation (65), except in this case the solution is for a general longitudinal coordinate. The solution is restricted to $\zeta<\psi<\frac{\zeta}{V_\ell}$. For $\psi<\zeta$, $c_{fcsd}=0$, because this corresponds to a time before a solute, released at the time zero, could reach the downstream location moving at the fastest advective (fracture) velocity. For $\psi>\frac{\zeta}{V_\ell}$, the solute concentration becomes steady, i.e., $c_{fcsd}(\zeta,\psi)=c_{fcsd}\left(\zeta,\frac{\zeta}{V_\ell}\right)$, because the last solutes, released at time zero, have reached the downstream location moving at the slowest (matrix) advective velocity. The result of the integration in Equation (77) is identical to Equation (66), with ζ_0 replaced by ζ.

The concentration field in the rock matrix, c_{mcs}, that evolves from a continuous source in the fracture given by the following superposition integral analogous to Equation (76),

$$c_{mcsd}(\eta,\zeta,\psi)=\int_0^{\psi} c_{md}(\eta,\zeta,\mu)\exp(-\lambda_d\mu)d\mu \tag{78}$$

where $c_{mcsd}=\frac{A_f\phi_f S_f R_f v_f}{\dot{M}}c_{mcs}$.

The function $c_{md}(\eta,\zeta,\sigma)$ is given in Equation (56). The integral in Equation (78) differs from the solute mass flux integral in Equation (69) because integration over the transverse coordinate, η, is not performed. The integration of Equation (78) is similar to that shown in Appendix I for the derivation of Equation (66). The result is,

$$
\begin{aligned}
c_{mcsd}(\zeta,\eta,\psi) = {} & \frac{\left\{(PeV-V_\ell)^2+4Pe\lambda_d\right\}^{\frac{1}{2}}+V_\ell}{2\left\{(PeV-V_\ell)^2+4Pe\lambda_d\right\}^{\frac{1}{2}}} \\
& \bullet \exp\left[-\frac{\zeta}{2Pe}\left\{(1-V_\ell)(PeV-V_\ell)+2Pe\lambda_d\right\}+\frac{\eta}{2}(PeV+V_\ell)\right] \\
& \bullet \exp\left(\left\{\frac{\zeta(1-V_\ell)+Pe\eta}{2Pe}\right\}\left\{(PeV-V_\ell)^2+4Pe\lambda_d\right\}^{\frac{1}{2}}\right) \\
& \bullet \operatorname{erfc}\left[\frac{\left\{(PeV-V_\ell)^2+4Pe\lambda_d\right\}^{\frac{1}{2}}(\psi-\zeta)+\zeta(1-V_\ell)+Pe\eta}{2\sqrt{Pe}\sqrt{\psi-\zeta}}\right] \\
& - \frac{\left\{(PeV-V_\ell)^2+4Pe\lambda_d\right\}^{\frac{1}{2}}-V_\ell}{2\left\{(PeV-V_\ell)^2+4Pe\lambda_d\right\}^{\frac{1}{2}}} \\
& \bullet \exp\left[-\frac{\zeta}{2Pe}\left\{(1-V_\ell)(PeV-V_\ell)+2Pe\lambda_d\right\}+\frac{\eta}{2}(PeV+V_\ell)\right] \\
& \bullet \exp\left(-\left\{\frac{\zeta(1-V_\ell)+Pe\eta}{2Pe}\right\}\left\{(PeV-V_\ell)^2+4Pe\lambda_d\right\}^{\frac{1}{2}}\right) \\
& \bullet \operatorname{erfc}\left[\frac{\left\{(PeV-V_\ell)^2+4Pe\lambda_d\right\}^{\frac{1}{2}}(\psi-\zeta)-\zeta(1-V_\ell)-Pe\eta}{2\sqrt{Pe}\sqrt{\psi-\zeta}}\right]
\end{aligned}
\qquad (79)
$$

for $\zeta \le \psi \le \frac{\zeta}{V_\ell}$. For $\psi < \zeta$, $c_{mcsd}(\eta,\zeta,\psi) = 0$ and for $\frac{\zeta}{V_\ell} < \psi$, the solution has achieved steady-state, $c_{mcsd}(\eta,\zeta,\psi) = c_{mcsd}\left(\eta,\zeta,\frac{\zeta}{V_\ell}\right)$.

The solutions in Equation (66) (with ζ_0 replaced by ζ) and Equation (79) may be compared with Equations (42) and (44) given in Tang et al. (1981) for concentrations from a continuous source in the fracture, Tang et al. (1981) derived solutions for a saturated system with no flow in the rock matrix both with and without with longitudinal dispersion in the fracture. The solutions in Equations (42) and (44) of Tang et al. (1981) are for the no dispersion case. The comparable case for the model presented here is obtained by setting $V = 0$ and $V_\ell = 0$, which assigns no flow in the matrix. Saturated conditions and full contact area imply $S_f = 1$, $S_m = 1$, and $A_r = 1$. The solution presented by Tang et al. (1981) also assumes no fine materials in the fracture, so the fracture porosity, ϕ_f, is 1. Note the following differences in mathematical terms between the present solution and Tang et al. (1981): $R_f \Rightarrow R$, $R_m \Rightarrow R'$, $D_m \Rightarrow D'$, $q_f \Rightarrow v$,

$\phi_m \Rightarrow \theta$, and $\frac{b}{2} \Rightarrow b$. Note also that Equation (42b) in Tang et al. (1981) contains a typographical error. The term $\frac{z}{2vAT'}$ contained in both complementary error functions in Equation (42b) of Tang et al. (1981) should be $\frac{Rz}{2vAT'}$. This can be seen from the solution presented here, Equation (66), when applied to the case with no flow in the matrix and from the derivation leading up to Equation (42b) in Tang et al. (1981). The solutions in Equations (66) and (79) are otherwise found to be in agreement with the solutions presented in Equations (42) and (44) of Tang et al. (1981).

4. Mathematical Solution – Matrix Solute Source

The general solution scheme is the same as described for the solution with a fracture solute source. The only difference in the formulation is in the initial conditions, as shown in Figure 1, which locates the solute source in the matrix.

4.1 Modified Initial Conditions for the Matrix Solute Source

The dimensionless form of the solute mass conservation equation for the fracture is given in Equation (29). The boundary condition given in Equation (32) is also unchanged. The initial condition for the matrix solute source case is

$$c_{fd}(\xi,0) = 0 \tag{80}$$

The dimensionless form of the solute mass conservation equation for the matrix is unchanged from the previous case, as given in Equation (34). The boundary conditions given in Equations (35) and (36) are also unchanged. The initial condition for the matrix solute source case is

$$\int_0^{\infty}\int_{-\infty}^{\infty} 2\left(\frac{A_f A_r}{b}\right)\phi_m S_m R_m c_m(x,z,0)\,dx\,dz = M_0 \tag{81}$$

where the total source mass = M_0 (see Figure 1b) and

$$c_m(x,z,0) = \frac{M_0 b}{2A_r A_f \phi_m S_m R_m}\delta(x-x_0)\delta(z) \tag{82}$$

where x_0 is the transverse coordinate of the solute source. Using Equation (28) for c_m in Equation (82) gives,

$$c_{md}(x,z,0) = \frac{S_f R_f b\ell}{2A_r \phi_m S_m R_m}\delta(x-x_0)\delta(z) \tag{83}$$

Using Equation (23) in Equation (83) gives

$$c_{md}(x,z,0) = \ell^2 \delta(x - x_0)\delta(z) = \delta(\eta - \eta_0)\delta(\xi) \tag{84}$$

Substituting Equation (28) for c_m in Equation (80) and using Equation (23) gives

$$\int_0^\infty \int_{-\infty}^{\infty} c_{md}(\eta,\xi,0)\, d\eta\, d\xi = 1 \tag{85}$$

4.2 Solution for the Laplace Transformed Matrix and Fracture Concentrations

Following the same strategy as used for the fracture solute source case, Equation (34) for the matrix concentration, with boundary conditions in Equations (35) and (36), are solved subject to the initial condition for a matrix source in Equation (84). Details concerning the development of the solution, obtained using the Laplace transform, are given in Appendix II. The solution for the Laplace transformed matrix concentration is given by,

For $\eta < \eta_0$

$$\begin{aligned}\hat{c}^{-}_{md}(\eta,\xi,s) = \hat{c}_{fd}(\xi,s)\exp\left[\left\{\frac{PeV}{2} - \sqrt{\left(\frac{PeV}{2}\right)^2 + sPe}\right\}\eta\right] \\ + \frac{Pe\,\delta(\xi)\exp\left[\left(\frac{PeV}{2} + \sqrt{\left(\frac{PeV}{2}\right)^2 + sPe}\right)(\eta - \eta_0)\right]}{2\sqrt{\left(\frac{PeV}{2}\right)^2 + sPe}} \\ - \frac{Pe\,\delta(\xi)\exp\left[\frac{PeV}{2}(\eta - \eta_0) - \left(\sqrt{\left(\frac{PeV}{2}\right)^2 + sPe}\right)(\eta + \eta_0)\right]}{2\sqrt{\left(\frac{PeV}{2}\right)^2 + sPe}}\end{aligned} \tag{86}$$

For $\eta > \eta_0$

$$\hat{c}^{+}_{md}(\eta,\xi,s)=\hat{c}_{fd}(\xi,s)\exp\left[\left\{\frac{PeV}{2}-\sqrt{\left(\frac{PeV}{2}\right)^2+sPe}\right\}\eta\right]$$
$$+\frac{Pe\delta(\xi)\exp\left[\left(\frac{PeV}{2}-\sqrt{\left(\frac{PeV}{2}\right)^2+sPe}\right)(\eta-\eta_0)\right]}{2\sqrt{\left(\frac{PeV}{2}\right)^2+sPe}} \qquad (87)$$
$$-\frac{Pe\delta(\xi)\exp\left[\frac{PeV}{2}(\eta-\eta_0)-\left(\sqrt{\left(\frac{PeV}{2}\right)^2+sPe}\right)(\eta+\eta_0)\right]}{2\sqrt{\left(\frac{PeV}{2}\right)^2+sPe}}$$

The solution for the Laplace transformed matrix concentration is then used to derive the solution of Equation (29) for the Laplace transformed fracture concentration, subject to the boundary condition given in Equation (32), the initial condition given in Equation (80) and the solution for $\hat{c}^{-}_{md}(\eta,\xi,s)$ in Equation (86). Details concerning the development of the solution, obtained using the Laplace transform, are given in Appendix II. The solution for the Laplace transformed fracture concentration is given by,

$$\hat{c}_{fd}(\xi,s)=H(\xi)e^{-s\xi}\exp\left[-\left(\frac{V}{2}+\sqrt{\frac{V^2}{4}+\frac{s}{Pe}}\right)(\xi+Pe\eta_0)\right] \qquad (88)$$

4.3 Inversion of the Laplace Transformed Solutions

As for the fracture solute source case, the transform to real time is performed using the convolution theorem. The details of the inversion are similar to those presented for the fracture solute source case in Section 3.2. The resulting solution is,

$$c_{fd}(\xi,\tau)=H(\xi)H(\tau-\xi)\left(\frac{\xi+Pe\eta_0}{2\sqrt{\pi}\sqrt{Pe}(\tau-\xi)^{3/2}}\right)\exp\left[-\left\{\frac{\xi+Pe\eta_0+PeV(\tau-\xi)}{2\sqrt{Pe}\sqrt{\tau-\xi}}\right\}^2\right] \qquad (89)$$

This solution, analogous to Equation (53) for the fracture solute source case, contains the additional variable η_0 defining the transverse position of the source in the matrix.

The transformation of the matrix concentration is performed using the convolution theorem and following a similar approach as used for the fracture solute source case. Note that the solution for the Laplace transformed matrix concentration is split into two

domains, for $\eta < \eta_0$ and for $\eta > \eta_0$ as given in Equations (86) and (88). However, the solution transformed to real time gives identical results for the two domains. The details of the inversion are similar to those presented for the fracture solute source case in Section 3.2. The resulting solution is,

$$
\begin{aligned}
c_{md}(\eta,\xi,\tau) = H(\xi)H(\tau-\xi)\left(\frac{\xi + Pe(\eta+\eta_0)}{2\sqrt{\pi}\sqrt{Pe}(\tau-\xi)^{3/2}}\right)\bullet \\
\exp\left[-\left\{\frac{\xi + Pe(\eta+\eta_0) + PeV(\tau-\xi)}{2\sqrt{Pe}\sqrt{\tau-\xi}}\right\}^2\right]\exp(PeV\eta) \\
+\frac{\sqrt{Pe}\delta(\xi)}{2\sqrt{\pi}\sqrt{\tau}}\bullet \\
\left[\exp\left\{-\left(\frac{\sqrt{Pe}(\eta-\eta_0)-\sqrt{Pe}V\tau}{2\sqrt{\tau}}\right)^2\right\}\right. \\
\left.-\exp\left\{-\left(\frac{\sqrt{Pe}(\eta+\eta_0)-\sqrt{Pe}V\tau}{2\sqrt{\tau}}\right)^2\right\}\exp\left[-PeV\eta_0\right]\right]
\end{aligned}
\tag{90}
$$

4.4 Cumulative Mass Arrivals at a Downstream Location

The same procedure as outlined for the fracture solute source case is used here, only using the concentration solutions for the matrix solute source case as given in Equations (89) and (90).

The cumulative mass flux in the fracture is found by performing the integration as given in Equation (65), using Equation (89) for c_{fd}. This integration is similar to that shown in Appendix I for the derivation of Equation (66). The result is,

$$\frac{M_f}{M_0}(\psi)=\frac{\exp\left\{-\frac{\zeta_0}{2Pe}\left\{(1-V_\ell)(PeV-V_\ell)+2Pe\lambda_d\right\}-\frac{\eta_0}{2}(PeV-V_\ell)\right\}}{2\left\{(PeV-V_\ell)^2+4Pe\lambda_d\right\}^{\frac{1}{2}}}\bullet$$

$$\left[\begin{array}{l}
\left(\left\{(PeV-V_\ell)^2+4Pe\lambda_d\right\}^{\frac{1}{2}}+V_\ell\right)\bullet \\
\exp\left[\frac{\zeta_0(1-V_\ell)+Pe\eta_0}{2Pe}\left\{(PeV-V_\ell)^2+4Pe\lambda_d\right\}^{\frac{1}{2}}\right]\bullet \\
\operatorname{erfc}\left\{\frac{\left\{(PeV-V_\ell)^2+4Pe\lambda_d\right\}^{\frac{1}{2}}(\psi-\zeta_0)+\zeta_0(1-V_\ell)+Pe\eta_0}{2\sqrt{Pe}\sqrt{\psi-\zeta_0}}\right\} \\
-\left(\left\{(PeV-V_\ell)^2+4Pe\lambda_d\right\}^{\frac{1}{2}}-V_\ell\right)\bullet \\
\exp\left[-\frac{\zeta_0(1-V_\ell)+Pe\eta_0}{2Pe}\left\{(PeV-V_\ell)^2+4Pe\lambda_d\right\}^{\frac{1}{2}}\right]\bullet \\
\operatorname{erfc}\left\{\frac{\left\{(PeV-V_\ell)^2+4Pe\lambda_d\right\}^{\frac{1}{2}}(\psi-\zeta_0)-\zeta_0(1-V_\ell)-Pe\eta_0}{2\sqrt{Pe}\sqrt{\psi-\zeta_0}}\right\}
\end{array}\right] \qquad (91)$$

for $\zeta_0 \le \psi \le \frac{\zeta_0}{V_\ell}$. For $\psi < \zeta_0$, $\frac{M_f}{M_0}(\psi)=0$ and for $\psi > \frac{\zeta_0}{V_\ell}$, $\frac{M_f}{M_0}(\psi)=\frac{M_f}{M_0}\left(\frac{\zeta_0}{V_\ell}\right)$.

The cumulative mass flux in the matrix is found by performing the integration as given in Equation (69), using Equation (90) for c_{md}. This integration is similar to that shown in Appendix I for the derivation of Equation (66). The result is,

$$\frac{M_m}{M_0}(\psi)=\frac{-V_\ell\exp\left[-\frac{\zeta_0}{2Pe}\{(1-V_\ell)(PeV-V_\ell)+2Pe\lambda_d\}-\frac{\eta_0}{2}\{PeV-V_\ell\}\right]}{4(VV_\ell-\lambda_d)\{(PeV-V_\ell)^2-4Pe\lambda_d\}^{\frac{1}{2}}}\bullet$$

$$\left[\begin{array}{l}
\left[4(VV_\ell-\lambda_d)-V\left(PeV+V_\ell-\{(PeV-V_\ell)^2-4Pe\lambda_d\}^{\frac{1}{2}}\right)\right]\bullet \\
\exp\left\{\frac{\{\zeta_0(1-V_\ell)+Pe\eta_0\}}{2Pe}\{(PeV-V_\ell)^2-4Pe\lambda_d\}^{\frac{1}{2}}\right\}\bullet \\
\operatorname{erfc}\left\{\frac{\{(PeV-V_\ell)^2-4Pe\lambda_d\}^{\frac{1}{2}}(\psi-\zeta_0)+\zeta_0(1-V_\ell)+Pe\eta_0}{2\sqrt{Pe}\sqrt{\psi-\zeta_0}}\right\} \\
+\left[4(VV_\ell-\lambda_d)-V\left(PeV+V_\ell+\{(PeV-V_\ell)^2-4Pe\lambda_d\}^{\frac{1}{2}}\right)\right]\bullet \\
\exp\left\{-\frac{\{\zeta_0(1-V_\ell)+Pe\eta_0\}}{2Pe}\{(PeV-V_\ell)^2-4Pe\lambda_d\}^{\frac{1}{2}}\right\}\bullet \\
\operatorname{erfc}\left\{\frac{\{(PeV-V_\ell)^2-4Pe\lambda_d\}^{\frac{1}{2}}(\psi-\zeta_0)-\zeta_0(1-V_\ell)-Pe\eta_0}{2\sqrt{Pe}\sqrt{\psi-\zeta_0}}\right\}
\end{array}\right]$$

$$\frac{-VV_\ell}{2(VV_\ell-\lambda_d)}\exp\{-V(\zeta_0-V_\ell\psi+Pe\eta_0)-\zeta_0\lambda_d\}\bullet$$

$$\operatorname{erfc}\left\{\frac{(PeV+V_\ell)(\psi-\zeta_0)-\zeta_0(1-V_\ell)-Pe\eta_0}{2\sqrt{Pe}\sqrt{\psi-\zeta_0}}\right\}$$

$$+\frac{H\left(\psi-\frac{\zeta_0}{V_\ell}\right)\exp\left(-\frac{\lambda_d\zeta_0}{V_\ell}\right)}{2}\bullet$$

$$\left[\begin{array}{l}
\operatorname{erfc}\left\{\frac{-\sqrt{Pe}\sqrt{V_\ell}}{2\sqrt{1-V_\ell}\sqrt{\zeta_0}}\left\{\eta_0+V(1-V_\ell)\frac{\zeta_0}{V_\ell}\right\}\right\} \\
-\exp(-PeV\eta_0)\operatorname{erfc}\left\{\frac{\sqrt{Pe}\sqrt{V_\ell}}{2\sqrt{1-V_\ell}\sqrt{\zeta_0}}\left\{\eta_0-V(1-V_\ell)\frac{\zeta_0}{V_\ell}\right\}\right\}
\end{array}\right] \qquad (92)$$

for $\zeta_0\le\psi\le\frac{\zeta_0}{V_\ell}$. For $\psi<\zeta_0$, $\frac{M_m}{M_0}(\psi)=0$ and for $\psi>\frac{\zeta_0}{V_\ell}$, $\frac{M_m}{M_0}(\psi)=\frac{M_m}{M_0}\left(\frac{\zeta_0}{V_\ell}\right)$.

The combined cumulative mass arrival at the downstream location is given by the sum of Equations (91) and (92). The result is,

$$\frac{M_f + M_m}{M_0}(\psi) = \frac{VV_\ell \exp\left[-\frac{\zeta_0}{2Pe}\left\{(1-V_\ell)(PeV - V_\ell) + 2Pe\lambda_d\right\} - \frac{\eta_0}{2}\left\{PeV - V_\ell\right\}\right]}{4(VV_\ell - \lambda_d)\left\{(PeV - V_\ell)^2 - 4Pe\lambda_d\right\}^{\frac{1}{2}}} \bullet$$

$$\left[\begin{array}{l}
\left[PeV - \left(1 - \frac{2\lambda_d}{VV_\ell}\right)\left(V_\ell - \left\{(PeV - V_\ell)^2 + 4Pe\lambda_d\right\}^{\frac{1}{2}}\right)\right] \bullet \\
\exp\left\{ \frac{\left\{\zeta_0(1-V_\ell) + Pe\eta_0\right\}}{2Pe}\left\{(PeV - V_\ell)^2 - 4Pe\lambda_d\right\}^{\frac{1}{2}}\right\} \bullet \\
\operatorname{erfc}\left\{ \frac{\left\{(PeV - V_\ell)^2 - 4Pe\lambda_d\right\}^{\frac{1}{2}}(\psi - \zeta_0) + \zeta_0(1-V_\ell) + Pe\eta_0}{2\sqrt{Pe}\sqrt{\psi - \zeta_0}}\right\} \\
+ \left[PeV - \left(1 - \frac{2\lambda_d}{VV_\ell}\right)\left(V_\ell + \left\{(PeV - V_\ell)^2 + 4Pe\lambda_d\right\}^{\frac{1}{2}}\right)\right] \bullet \\
\exp\left\{ -\frac{\left\{\zeta_0(1-V_\ell) + Pe\eta_0\right\}}{2Pe}\left\{(PeV - V_\ell)^2 - 4Pe\lambda_d\right\}^{\frac{1}{2}}\right\} \bullet \\
\operatorname{erfc}\left\{ \frac{\left\{(PeV - V_\ell)^2 - 4Pe\lambda_d\right\}^{\frac{1}{2}}(\psi - \zeta_0) - \zeta_0(1-V_\ell) - Pe\eta_0}{2\sqrt{Pe}\sqrt{\psi - \zeta_0}}\right\}
\end{array}\right]$$

$$\frac{-VV_\ell}{2(VV_\ell - \lambda_d)} \exp\left\{-V(\zeta_0 - V_\ell\psi + Pe\eta_0) - \zeta_0\lambda_d\right\} \bullet$$

$$\operatorname{erfc}\left\{ \frac{(PeV + V_\ell)(\psi - \zeta_0) - \zeta_0(1-V_\ell) - Pe\eta_0}{2\sqrt{Pe}\sqrt{\psi - \zeta_0}}\right\}$$

$$+ \frac{H\left(\psi - \frac{\zeta_0}{V_\ell}\right)\exp\left(-\frac{\lambda_d\zeta_0}{V_\ell}\right)}{2} \bullet$$

$$\left[\begin{array}{l}
\operatorname{erfc}\left\{ \frac{-\sqrt{Pe}\sqrt{V_\ell}}{2\sqrt{1-V_\ell}\sqrt{\zeta_0}}\left\{\eta_0 + V(1-V_\ell)\frac{\zeta_0}{V_\ell}\right\}\right\} \\
- \exp(-PeV\eta_0)\operatorname{erfc}\left\{ \frac{\sqrt{Pe}\sqrt{V_\ell}}{2\sqrt{1-V_\ell}\sqrt{\zeta_0}}\left\{\eta_0 - V(1-V_\ell)\frac{\zeta_0}{V_\ell}\right\}\right\}
\end{array}\right]$$

for $\zeta_0 \le \psi \le \frac{\zeta_0}{V_\ell}$. For $\psi < \zeta_0$, $\frac{M_f + M_m}{M_0}(\psi) = 0$ and for $\psi > \frac{\zeta_0}{V_\ell}$,

$$\frac{M_f + M_m}{M_0}(\psi) = \frac{M_f + M_m}{M_0}\left(\frac{\zeta_0}{V_\ell}\right) .$$

For a non-decaying solute ($\lambda = 0$), the result in Equation (93) simplifies to,

$$\frac{M_f + M_m}{M_0}(\psi) = \frac{1}{2}\exp\{-V(\zeta_0 - V_\ell\psi + Pe\eta_0)\}\bullet$$
$$\operatorname{erfc}\left\{\frac{\zeta_0 - V_\ell\psi + Pe\eta_0 - PeV(\psi-\zeta_0)}{2\sqrt{Pe}\sqrt{\psi-\zeta_0}}\right\}$$
$$+\frac{1}{2}\operatorname{erfc}\left\{\frac{\zeta_0 - V_\ell\psi + Pe\eta_0 + PeV(\psi-\zeta_0)}{2\sqrt{Pe}\sqrt{\psi-\zeta_0}}\right\} + \frac{1}{2}H\left(\psi - \frac{\zeta_0}{V_\ell}\right)\bullet \qquad (94)$$
$$\left[\begin{array}{l}\operatorname{erfc}\left\{\dfrac{-\sqrt{Pe}\sqrt{V_\ell}}{2\sqrt{1-V_\ell}\sqrt{\zeta_0}}\left\{\eta_0 + V(1-V_\ell)\dfrac{\zeta_0}{V_\ell}\right\}\right\} \\ -\exp(-PeV\eta_0)\operatorname{erfc}\left\{\dfrac{\sqrt{Pe}\sqrt{V_\ell}}{2\sqrt{1-V_\ell}\sqrt{\zeta_0}}\left\{\eta_0 - V(1-V_\ell)\dfrac{\zeta_0}{V_\ell}\right\}\right\}\end{array}\right]$$

4.5 Concentration from a Continuous Point Source

The concentration field that evolves from a continuous point source in the matrix, c_{fcs}, may be derived through the superposition integral in Equation (76) as done for a continuous point source in the fracture. The results of this calculation are the same as those given in Equation (91), with ζ_0 replaced by ζ and for $\frac{\zeta}{V_\ell} < \psi$ and that the solution has achieved steady-state, $c_{fcsd}(\zeta,\psi) = c_{fcsd}\left(\zeta, \frac{\zeta}{V_\ell}\right)$.

Similarly, the concentration field in the rock matrix, c_{mcs}, that evolves from a continuous source in the fracture given by the superposition integral in Equation (78). The function $c_{md}(\eta,\zeta,\sigma)$ is given in Equation (90). As before, the integral in Equation (78) differs from the solute mass flux integral in Equation (69) because integration over the transverse coordinate, η, is not performed. The integration of Equation (78) is similar to that shown in Appendix I for the derivation of Equation (66). The result is,

$$c_{mcsd}(\zeta,\eta,\psi)=\frac{\exp\left[\frac{\zeta}{2Pe}\left[(1-V_\ell)(PeV+V_\ell)-2Pe\lambda_d\right]+\frac{(\eta+\eta_0)}{2}(PeV+V_\ell)+PeV\eta\right]}{4\left\{(PeV-V_\ell)^2+4Pe\lambda_d\right\}^{\frac{1}{2}}}$$

$$\bullet\left\{\begin{array}{l}\left[\left\{(PeV-V_\ell)^2+4Pe\lambda_d\right\}^{\frac{1}{2}}+V_\ell\right]\\ \bullet\exp\left(\frac{\zeta(1-V_\ell)+Pe(\eta+\eta_0)}{2Pe}\left\{(PeV+V_\ell)^2+4Pe\lambda_d\right\}^{\frac{1}{2}}\right)\\ \bullet\operatorname{erfc}\left[\frac{\left\{(PeV+V_\ell)^2+4Pe\lambda_d\right\}^{\frac{1}{2}}(\psi-\zeta)+\zeta(1-V_\ell)+Pe(\eta+\eta_0)}{2\sqrt{Pe}\sqrt{\psi-\zeta}}\right]\\ -\left[\left\{(PeV-V_\ell)^2+4Pe\lambda_d\right\}^{\frac{1}{2}}-V_\ell\right]\\ \bullet\exp\left(-\frac{\zeta(1-V_\ell)+Pe(\eta+\eta_0)}{2Pe}\left\{(PeV+V_\ell)^2+4Pe\lambda_d\right\}^{\frac{1}{2}}\right)\\ \bullet\operatorname{erfc}\left[\frac{\left\{(PeV+V_\ell)^2+4Pe\lambda_d\right\}^{\frac{1}{2}}(\psi-\zeta)-\zeta(1-V_\ell)-Pe(\eta+\eta_0)}{2\sqrt{Pe}\sqrt{\psi-\zeta}}\right]\end{array}\right\} \quad (95)$$

for $\zeta\le\psi\le\frac{\zeta}{V_\ell}$. For $\psi<\zeta$, $c_{mcsd}(\eta,\zeta,\psi)=0$ and for $\frac{\zeta}{V_\ell}<\psi$, the solution has achieved steady-state, $c_{mcsd}(\eta,\zeta,\psi)=c_{mcsd}\left(\eta,\zeta,\frac{\zeta}{V_\ell}\right)$.

5. Solution Behavior of the Analytical Model and Comparisons with Numerical Simulations

Numerical simulations were performed using TOUGH2 simulation tools (Pruess et al., 1999) to compare with the analytical model. Flow was computed using the TOUGH2 unsaturated flow module, EOS9 (Pruess et al., 1999), and transport was computed using the T2R3D module (Wu et al., 1996). The numerical model was developed to approximate the model restrictions concerning spatially uniform flow and saturation within the fracture and within the matrix. The relative permeability functions for the fracture and matrix are linear and the capillary pressures are assigned fixed values to drive a uniform cross-flow. The dimensions of the model are 100 m in the direction of flow and 12.7 m in the transverse direction, with a fracture aperture of 0.001 m. For both fracture and matrix solute source cases, the sources are located at the top of the model. For the matrix solute source case, the source is approximately 1 m in the transverse direction from the primary fracture-matrix interface. The numerical grid utilizes more refined gridding in the transverse direction near the primary fracture-matrix interface, ranging from 0.02 m to about 1.1 m. The gridding in the longitudinal direction is a

uniform 1 m spacing. To accommodate a cross-flow, a second fracture is included on the opposite side of the model. This fracture is sufficiently far from the primary fracture such that only a negligible amount of tracer released in the different cases was able reach the right hand side of the model.

The fracture velocity in the cases investigated here is approximately 10,000 times faster than the matrix velocity. The fracture velocity is about 2700 m/yr, resulting in a travel time in the fracture of about 13 days. The travel time in the matrix is approximately 367 years. Two flow fields with different levels of transverse flow (from fracture to matrix) were investigated for the fracture solute source case. One flow field has a low cross-flow velocity of about 0.1 percent of the matrix longitudinal velocity. A second flow field has a higher cross-flow velocity of about 2 percent of the matrix longitudinal velocity. Only the low cross-flow case was investigated for the matrix solute source case because very little fracture interaction occurs for the high cross-flow case. For each case, transport under three different Peclet numbers (Equation (30)), ranging over three orders of magnitude, were investigated. The Peclet number was varied by changing the diffusion coefficient. Note that although longitudinal and transverse dispersion were not included in the numerical model, diffusion was modeled as isotropic. This differs from the analytical model, which only accounts for transverse diffusion.

For the high cross-flow case, water was introduced as a distributed source along the length of the fracture to maintain the uniform saturation conditions in the fracture and matrix. This additional source of water was introduced because the fracture saturation is significantly depleted by the cross-flow. This depletion leads to a reduced cross-flow into the matrix because the linear relative permeability function used for the fracture is isotropic. The fracture relative permeability is used to model the permeability along the fracture direction as a function of saturation. However, it is expected that the permeability transverse to the fracture direction is much less sensitive to saturation. Therefore, the transverse flow rate is expected to remain relatively constant, even though the fracture saturation drops off with distance along the fracture. This also presumes that the fracture capillary pressure is constant over the range of fracture saturations. The fracture saturation itself should decrease with distance along the fracture, but the introduction of water along the flow path forces the fracture saturation to remain constant. However, as shown in Section 5.4, transport is found to be insensitive to fracture saturation. Thus, the significance of the introduced water is to maintain a constant saturation in the matrix.

Table 1 presents the flow conditions used for the comparison calculations. Two flow fields were investigated that have different levels of transverse flux, or cross-flow, between the fracture and the matrix. The radionuclide source in the fracture lies at a z-coordinate of zero. For the case of a source term in the matrix, the source lies at a z-coordinate of zero and an x-coordinate of 0.988 m from the fracture-matrix interface. Transport properties are shown in Table 2. Three different matrix diffusion coefficients were used to investigate the effects of variations in Peclet number.

Table 1. Flow results for low and high cross-flow cases.

Flow Conditions	Low Cross-Flow	High Cross-Flow
fracture flow rate, Q_f (m^2/s)	1.89×10^{-9}	1.96×10^{-9}
matrix flux, q_m (m/s)	6.97×10^{-10}	7.02×10^{-10}
transverse flux, q_{fm} (m/s)	7.11×10^{-13}	1.42×10^{-11}
fracture saturation, S_f	0.0219	0.0227
matrix saturation, S_m	0.808	0.814

Table 2. Parameter values used for the transport calculations.

Transport and Source Parameters	Values
fracture porosity, ϕ_f	1
matrix porosity, ϕ_m	0.1
fracture retardation, R_f	1
matrix retardation, R_m	1
fracture aperture, b (m)	0.001
fracture-matrix area reduction factor, A_r	1
matrix diffusion coefficient, D_m (m^2/s)	3.2×10^{-10} ; 3.2×10^{-11} ; 3.2×10^{-12}
longitudinal distance, z_0 (m)	100
solute mass released, M_0 (kg)	22.7

5.1 Comparisons of Cumulative Mass Arrival

The normalized cumulative mass arrival curves for the low-Peclet-number scenarios are shown in Figure 2. The fractional breakthrough refers to the fraction of solute initially released that has arrived at the 100-m boundary. The analytical model is based on Equation (72) for fracture solute source and Equation (94) for the matrix solute source. The low Peclet number case shows some effects of longitudinal diffusion at the long-time tails of the breakthrough curves for the numerical model. The effects of cross-flow are seen to increase arrival times over most of the curve. For the matrix solute source case, the analytical model shows that approximately 30 percent of the mass arrives at the matrix travel time of 367 years. This fraction of the solute did not interact with the fracture flow. The analytical and numerical models show generally good agreement, with the matrix solute source case having somewhat larger discrepancies. This may be attributed to the coarser gridding in the numerical model at the location where the solute is released, resulting in delayed transport in the numerical model.

The normalized cumulative mass arrival curves for the medium-Peclet-number scenarios are shown in Figure 3. As for the low-Peclet number case, some effects of longitudinal diffusion are seen at the long-time tails of the pronounced than in the low-Peclet number cases, although these effects are smaller than for the low-Peclet-number cases. The initial breakthrough times for the fracture solute source cases are shorter than for the low-Peclet-number cases, with arrivals starting at less than 10 years. The effect is the opposite for the matrix solute source case, with initial arrivals starting at about 100 years

and nearly 80 percent of the solute arrives at the matrix travel time of 367 years. In general, the effects of cross-flow and solute source location are seen to result in greater differences in the cumulative arrival curves than for the low-Peclet-number cases.

The normalized cumulative mass arrival curves for the high-Peclet-number cases are shown in Figure 4. The effects of longitudinal diffusion are seen to be less here than for the other Peclet-number cases. The initial breakthrough times for the fracture solute source cases are the shortest of any of the cases, starting at less than 1 year. For the matrix solute source case, all of the solute arrives at the matrix travel time of 367 years. The effects of cross-flow and solute source location are most pronounced for the high-Peclet-number cases. Differences between the analytical and numerical models for the fracture solute source cases are slightly larger at high Peclet numbers. These differences indicate the effects discretization in the numerical model.

5.2 Comparisons of Concentration Distributions in the Fracture

Figure 5 shows the concentration profiles in the fracture for an instantaneous fracture solute source, low cross-flow, and the three values for Peclet number. The solutions are found to be in reasonable agreement, with discrepancies increasing with Peclet number. For the higher-Peclet number cases, the profiles are at times following breakthrough. Figures 6 and 7 show the comparisons of the higher-Peclet number cases at earlier times. These figures show that the numerical and analytical models are significantly different in terms of the concentration profiles at early times. These differences are attributed to the numerical approximations inherent in the particular spatial and temporal discretizations used in the numerical model. The concentration profiles are found to show much larger discrepancies than found in the corresponding cumulative mass arrival curves in Figures 3 and 4.

5.3 Comparisons of Concentration Distributions in the Matrix

Figure 8 shows a sequence of longitudinal concentration profiles at successively larger distances from the fracture-matrix interface, all at 13 years for an instantaneous fracture solute source and a Peclet number of 37. At larger longitudinal distances, the concentrations are monotonically decreasing with increasing distance into the matrix. This indicates diffusive solute flux into the matrix from the fracture. Lower concentrations are found for the profiles nearest the fracture at lower longitudinal coordinates, indicating diffusion of the solute from the matrix back into the fracture. Figure 9 shows the comparison of matrix concentrations as a contour map. The effect of clean water following the tracer mass is seen near the fracture at longitudinal distances less than about 20 m. The analytical model shows a sharp trailing edge at about 3.5 m which represents the slowest travel in the model. The numerical model shows a more diffuse edge due to the effects of longitudinal matrix diffusion.

A sequence of longitudinal concentration profiles at successively larger distances from the fracture-matrix interface is given in Figure 10. As for Figure 8, the profiles are all at 13 years for a fracture solute source, but the Peclet number in this case is 370, as

compared with a Peclet number of 37 in Figure 8. The results at a higher Peclet number show a similar pattern with the low Peclet number case, with the peak concentration in the first matrix cells along the fracture (x = 0.0105 m) about twice as far downstream as in the low Peclet number case. Figure 11 shows the more limited diffusion into the matrix for the higher Peclet number conditions.

Figure 12 shows a further progression of the same patterns at a higher Peclet number of 3700. In this case, the peak concentration in the first matrix cells along the fracture (x = 0.0105 m) has exited the model. Figure 13 shows that diffusive penetration into the matrix is limited to about 20 cm compared with about 1.8 m for the case with a Peclet number of 37 and about 0.6 m for the case with a Peclet number of 370. In general, agreement between the analytical and numerical models appears to be better for lower Peclet numbers.

5.4 Sensitivities of the Solution

The results presented show that the solution is sensitive to the Peclet number (Equation (30)), cross-flow velocity ratio (Equation (31)), and the location of the source. The solution sensitivity to the cross-flow velocity ratio and source location increase with Peclet number because averaging over the different transport velocities in the fracture and matrix is reduced at higher Peclet number. Sensitivity calculations using the analytical model have shown expected trends with changes in fracture flux, matrix flux, matrix porosity, matrix saturation, matrix retardation, matrix diffusion, and the fracture-matrix area reduction factor. Breakthrough times are reduced for higher fracture flux and matrix flux and for lower matrix porosity, matrix saturation, matrix retardation, matrix diffusion, and fracture-matrix area reduction factor.

Somewhat surprisingly, breakthrough times are not sensitive to fracture porosity, fracture saturation, fracture retardation, and fracture aperture over a fairly wide range. These sensitivity studies assume that the fracture flux fracture-matrix area reduction factor are not affected by changes in these properties. The product of these factors appear in the definitions of fracture velocity and the length scale. Although changes in these factors directly influence the transport velocity in the fracture, they also influence the effective fracture water volume per unit fracture-matrix interface area. For example a reduction in fracture water saturation leads to higher fracture velocities if all other factors remain the same. However, the reduction in fracture saturation also leads to a smaller fracture water volume per unit fracture-matrix interface area, resulting in greater fracture-matrix interaction. The opposing effects nearly balance, resulting in breakthrough times that are insensitive to these factors. Sensitivity to these factors begins to increase when the dimensionless downstream distance (Equation (63)) falls below 2×10^4. A calculation showing the effects of a one order of magnitude decrease in fracture porosity is given in Figure 14. Although the numerical model solution shows a slightly earlier breakthrough for lower fracture porosity, this is attributed to numerical discretization effects resulting from fracture velocities that are 10 times larger than for the base case.

5.5 Effects of Longitudinal Dispersion

Longitudinal dispersion is not included in the analytical model to simplify the solution to the governing equations. The effects of dispersion are caused primarily by smaller-scale velocity fluctuations not captured in the analytical or numerical flow fields. Dispersion is also caused by molecular diffusion, but this component is typically not a significant factor for field-scale transport problems. Dispersion may be modeled using the numerical solution method; the results with a dispersivity of 10 m is shown in Figure 14. The dispersivity length scale is only used for transport in the fracture. Dispersion in the matrix is relatively small because of the small velocities in the matrix and the smaller dispersivities characteristic of matrix flow. The figure shows that dispersion leads to reduced arrival times, however, the effects are not large compared with other sensitivities. The figure shows a comparison against the analytical model with an area reduction factor of 0.8 compared with a factor of 1. This is seen to result in a breakthrough curve close to the case with dispersion. The relatively small sensitivity to dispersion is primarily a result of the dispersion caused by fracture-matrix interaction, which is explicitly represented in both the analytical and numerical models. Thus, additional dispersion strictly for fracture transport appears to be a smaller component of the overall dispersion in this case. Clearly, conditions defining transport in the fracture and matrix and conditions that influence fracture-matrix interaction may significantly affect the relative contributions to dispersion. However, given the uncertainties that are generally associated with transport problems in fractured rock, the inclusion of a dispersion term may be of limited value when explicitly treating fracture and matrix transport.

6. Discussion

Standard numerical solutions of the governing equations are found to be quantitatively consistent with solutions from the analytical model. This agreement lends support to the use of numerical simulation methods for transport in fractured rock. The solutions presented indicate that discretization errors for numerical solutions of transport in fractured rock are more significant for cases with high Peclet numbers, that is, as the time scale for diffusive exchange becomes long in comparison with the time scale for advective transport through the fracture. This is partially a result of the finite spatial resolution for fracture-matrix interaction which leads to an underestimate of the diffusive exchange between the fracture and matrix for the initial solute penetrating a fracture. In the analytical model, this exchange is captured with infinite resolution that more effectively attenuates the initial solute penetration. The comparison between the numerical and analytical models also shows that the predictions of concentration may have errors substantially larger than those found for the corresponding cumulative mass.

The solution for cumulative mass is found to be insensitive to fracture aperture, porosity, saturation, and retardation. Note that for the single-fracture model, the porosity refers to the ratio of the fracture void volume to the fracture volume. Thus, a “clean” fracture would have a porosity of 1, and lower porosities result from materials that may fill the fracture. For a fracture continuum, the fracture porosity is often taken to be the fracture

void volume divided by the rock bulk volume. This definition of fracture porosity is affected by the fracture frequency as well as the aperture and presence of fracture filling materials. The extension of the sensitivity results to a fracture continuum suggest that the sensitivity to fracture porosity is low provided that the fracture frequency does not vary. Transport sensitivity to fracture frequency is expected because this affects the quantity of flow per fracture. Note, however, that the single-fracture model is only applicable to a fracture continuum provide that the fracture spacing is sufficiently large such that transport interactions between fractures are negligible.

A number of specific geometric and process restrictions have been used to define the problem as discussed in the introduction. Of these, the first two are most likely to result in serious errors in applying the model presented here. The condition of steady, uniform flow is not always appropriate for unsaturated flow in fractured rock. Unsaturated flow is frequently linked to unsteady infiltration boundary conditions and the weak capillary forces common to unsaturated fracture flow may allow deep penetration of transient flows. In such situations, transient flow will result in faster solute transport (assuming the solute is introduced during the transient flow period) than expected based on the solutions presented here if the flow rate is assigned the time-averaged value. Similarly, average flow rates under steady flow conditions may underestimate or overestimate transport rates resulting from nonuniform flow conditions. The cross-flow is represented as a constant velocity in the transport model, although this can only be approximately true near the fracture; symmetry requires that this velocity goes to zero at the midpoint between fractures. The flow and saturation fields may be approximated as spatially uniform if water flux between the fracture and matrix is small compared with the longitudinal flux in either domain. Therefore, the application of this model to any particular problem requires an assessment of the model's suitability relative to the expected flow behavior.

The condition of an infinite domain in the transverse direction is not appropriate when the transport is affected by the presence of multiple fractures. The analytical solutions presented here will initially be accurate if the other conditions are suitable for the problem. However, after sufficient time has elapsed for the solute to migrate laterally such that it is affected by the presence of more than one fracture, the solutions become increasingly inaccurate. The solutions can be accurate over the entire transport problem if the time scale for longitudinal transport of solute through the system is sufficiently short compared with the time scale for lateral migration between fractures. The effects of multiple fractures have been investigated for a transport in a fractured rock for the case where advective transport is limited to the fractures (Sudicky and Frind 1982).

7. Conclusions

A set of analytical solutions are presented for transport in a single fracture through a porous rock matrix with global flow in both the fracture and matrix, as well as advective and diffusive exchange between the fracture and rock matrix. The solutions are derived for instantaneous point sources in either the fracture or the rock matrix. Integrals of these solutions for cumulative mass arrivals at a downstream location and the evolution of

concentrations from a continuous point source are also derived. The solutions for a continuous source in the fracture are found to reduce to the no-dispersion case derived by Tang et al. (1981) for a continuous source in the fracture of a saturated system where flow occurs exclusively in the fracture.

Comparisons between the analytical model and numerical simulation methods shows the effects of numerical approximations as well as restrictions used in the analytical model. The comparison of analytical and numerical models indicates that numerical discretization effects are generally more significant for predictions of concentrations than for predictions of cumulative arrival distributions. Also, discretization effects are found to result in greater differences between the analytical and numerical models as Peclet number increases. The effects of the restriction of no dispersion in the analytical model were investigated through numerical solutions, which show that arrival times are reduced by dispersion. The analytical and numerical model results also show that overall dispersion of tracer arrivals in the case investigated is dominated by the fracture-matrix interaction, which is explicitly represented in the analytical model.

Sensitivity studies with the analytical model show that the solution is sensitive to changes in Peclet number, and shows increasing sensitivity to cross-flow velocity and source configuration with increasing Peclet number. Sensitivity to fracture porosity, fracture water saturation, fracture retardation factor, and fracture aperture are found to be small for large values of the dimensionless longitudinal distance. These factors affect both advective velocity in the fracture and fracture-water contact with the rock matrix. The opposing effects of these factors on advective velocity and fracture-matrix interaction for solute transport lead to the predicted low sensitivity.

This work was supported by the Director, Office of Science, Office of Basic Energy Sciences, of the U.S. Department of Energy under Contract No. DE-AC03-76SF00098.

Notation

Primary Variables

A_f = fracture cross-sectional area orthogonal to the z axis (L^2)

A_r = fracture-matrix interface area reduction factor (-)

A_{vfm} = fracture-matrix interface area/unit fracture volume (1/L)

b fracture aperture (L)

c_f solute mass concentration in fracture water (M/L^3)

c_{fa} sorbed concentration; mass of sorbed solute per unit mass of rock (-)

c_{fcs} fracture concentration field from a continuous point source (M/L^3)

c_m solute mass concentration in matrix water (M/L^3)

c_{ma} solute sorbed concentration expressed as mass of sorbed solute per unit mass of

rock matrix (-)

c_{mcs} matrix concentration field from a continuous point source (M/L^3)

D_m matrix diffusion coefficient (L^2/T)

K_{df} linear sorption coefficient (L^3/M)

K_{dm} linear sorption coefficient in the rock matrix (L^3/M)

M_0 initial mass of solute (including solute sorbed) (M)

$\dot{M} = \frac{\partial M}{\partial \tau}$ solute mass release rate from a continuous source (M/T)

Q_f volumetric flow rate per unit fracture depth (*y*-direction) through the representative fracture volume (L^2/T)

q_f fracture water flux (fracture water flow rate per unit fracture area) (L/T)

q_{fm} fracture-matrix flow rate per unit bulk area in *x* direction (L/T)

q_m matrix water flow rate per unit bulk area (in *z* direction) (L/T)

S_f fracture water saturation (fracture water volume per unit fracture volume) (-)

S_m matrix water saturation (matrix water volume per unit matrix bulk volume) (-)

t time (T)

x horizontal coordinate (L)

z vertical coordinate (L)

ϕ_f fracture porosity (fracture pore volume per unit fracture volume) (-)

ϕ_m matrix porosity (matrix pore volume per unit matrix bulk volume) (-)

λ decay constant for the radioactive solute (1/T)

ρ_{bf} rock mass available for sorption per unit fracture volume (M/L^3)

ρ_{bm} rock mass per unit bulk volume (M/L^3)

Derived Variables

$c_{fcsd} = \frac{A_f \phi_f S_f R_f v_f}{\dot{M}} c_{fcs}$, dimensionless fracture concentration from a continuous point source (-)

$c_{mcsd} = \frac{A_f \phi_f S_f R_f v_f}{\dot{M}} c_{mcs}$, dimensionless matrix concentration from a continuous point source(-)

$c_{fd} = \frac{A_f \phi_f S_f R_f \ell}{M_0} c_f$, dimensionless fracture concentration from an instantaneous point source (-)

$c_{md} = \frac{A_f \phi_f S_f R_f \ell}{M_0} c_m$, dimensionless matrix concentration from an instantaneous point source (-)

$\hat{c}_{md}$, Laplace transformed dimensionless matrix concentration (-)

$\hat{c}_{fd}$, Laplace transformed dimensionless fracture concentration (-)

$\hat{c}^{-}_{md}(\eta,\xi,s)$, Laplace transformed dimensionless matrix concentration (-) for $\eta < \eta_0$ with a matrix solute source

$\hat{c}^{+}_{md}(\eta,\xi,s)$, Laplace transformed dimensionless matrix concentration (-) for $\eta > \eta_0$ with a matrix solute source

$D^*_m = \dfrac{D_m}{R_m}$, effective matrix diffusion coefficient (L^2/T)

$\ell = \dfrac{b}{2A_r}\dfrac{\phi_f S_f R_f}{\phi_m S_m R_m}$, length scale (-)

$M_f(T)$, cumulative mass arrivals in the fracture (M)

$M_m(T)$, cumulative mass arrivals in the matrix (M)

$Pe = \dfrac{v^*_f \ell}{D^*_m}$, Peclet number (-)

$R_f = 1 + \dfrac{\rho_{bf} K_{df}}{\phi_f S_f}$, retardation coefficient in for transport in the fracture (-)

$R_m = 1 + \dfrac{\rho_{bm} K_{dm}}{\phi_m S_m}$, retardation coefficient for transport in the matrix (-)

s , Laplace transform variable (-)

T ; time of observation (T)

$v_f = \dfrac{Q_f}{b\phi_f S_f R_f}$, advective transport velocity in the fracture (L/T)

$v_{fm} = \dfrac{q_{fm}}{\phi_m S_m R_m}$, advective transport velocity in the matrix (x-direction) (L/T)

$v^*_f = v_f - v_m$ (L/T)

$v_m = \dfrac{q_m}{\phi_m S_m R_m}$, advective transport velocity in the matrix in the z direction (L/T)

$V = \dfrac{v_{fm}}{v^*_f}$, velocity ratio for cross-flow in the matrix (-)

$V_\ell = \dfrac{v_m}{v_f}$, velocity ratio for longitudinal flow in the matrix (-)

$\chi = s + \dfrac{PeV^2}{4}$ (-)

$\eta = \dfrac{x}{\ell}$, dimensionless transverse distance (-)

$\lambda_d = \frac{\lambda \ell}{v_f}$, dimensionless decay rate (-)

$\mu = \psi - \sigma$ (-)

$\sigma = \frac{v_f t}{\ell}$, dimensionless time (-)

$\varsigma = z - v_m t$, longitudinal coordinate in reference frame moving at the matrix velocity (L/T)

$\tau = \frac{v_f^* t}{\ell}$, dimensionless time in reference frame moving at the matrix velocity (-)

$\xi = \frac{\varsigma}{\ell}$, dimensionless longitudinal coordinate for reference frame moving at the matrix velocity (-)

$\psi = \frac{v_f T}{\ell}$, dimensionless observation time (-)

$\zeta_0 = \frac{z_0}{\ell}$ dimensionless longitudinal distance (-)

Special Functions

$\delta(\xi)$ = delta function
$H(\xi)$ = step function

References

Abramowitz, M. and Stegun, I.A., eds. 1972. *Handbook of Mathematical Functions with Formulas, Graphs, and Mathematical Tables.* National Bureau of Standards, Applied Mathematics Series. 55, 1046. Washington, D.C.: U.S. Department of Commerce.

Doughty, C. 1999. "Investigation of Conceptual and Numerical Approaches for Evaluating Moisture, Gas, Chemical, and Heat Transport in Fractured Unsaturated Rock." *Journal of Contaminant Hydrology, 38,* (1-3), 69-106. New York, New York: Elsevier.

Ho, C.K. 2001. "Dual-Porosity vs. Dual-Permeability Models of Matrix Diffusion in Fractured Rock." *"Back to the Future - Managing the Back End of the Nuclear Fuel Cycle to Create a More Secure Energy Future," Proceedings of the 9th International High-Level Radioactive Waste Management Conference (IHLRWM), Las Vegas, Nevada, April 29-May 3, 2001.* La Grange Park, Illinois: American Nuclear Society.

Liu, H.H.; Doughty, C.; and Bodvarsson, G.S. 1998. "An Active Fracture Model for Unsaturated Flow and Transport in Fractured Rocks." *Water Resources Research, 34,* (10), 2633-2646. Washington, D.C.: American Geophysical Union.

Pruess, K.; Oldenburg, C.; and Moridis, G. 1999. TOUGH2 User's Guide, Version 2.0, Lawrence Berkeley National Laboratory Report LBNL-43134.

Sudicky, E.A. and Frind, E.O. 1982. "Contaminant Transport in Fractured Porous Media: Analytical Solutions for a System of Parallel Fractures." *Water Resources Research, 18,* (6), 1634-1642. Washington, D.C.: American Geophysical Union.

Tang, D.H.; Frind, E.O.; and Sudicky, E.A. 1981. "Contaminant Transport in Fractured Porous Media: Analytical Solution for a Single Fracture." *Water Resources Research, 17,* (3), 555-564. Washington, D.C.: American Geophysical Union.

Wu, Y.S.; Ahlers, C.F.; Fraser, P.; Simmons, A.; and Pruess, K. 1996. Software Qualification of Selected TOUGH2 Modules, Lawrence Berkeley National Laboratory Report LBNL-39490.

Appendix I – Derivation of Cumulative Mass Arrival in the Fracture From a Fracture Solute Source

The derivation of Equation (66) uses the new variables defined in Equations (59), (63), and (64) in Equation (53) for c_{fd}. This gives,

$$c_{fd}(\zeta_0,\sigma)=H(\zeta_0-V_\ell\sigma)H(\sigma-\zeta_0)\frac{\zeta_0-V_\ell\sigma}{2\sqrt{\pi}\sqrt{Pe}(\sigma-\zeta_0)^{\frac{3}{2}}}\exp\left[-\left\{\frac{PeV(\sigma-\zeta_0)+\zeta_0-V_\ell\sigma}{2\sqrt{Pe}\sqrt{\sigma-\zeta_0}}\right\}^2\right] \quad \text{(I-1)}$$

The step functions define range of σ : $\zeta_0 \le \sigma \le \frac{\zeta_0}{V_\ell}$; this with Equation (I-1) in

Combining Equation (I-1) with Equation (65) gives,

$$\frac{M_f}{M_0}(\psi)=\int_{\zeta_0}^{\psi}\frac{\zeta_0-V_\ell\sigma}{2\sqrt{\pi}\sqrt{Pe}(\sigma-\zeta_0)^{\frac{3}{2}}}\exp\left[-\left\{\frac{PeV(\sigma-\zeta_0)+\zeta_0-V_\ell\sigma}{2\sqrt{Pe}\sqrt{\sigma-\zeta_0}}\right\}^2\right]\exp(-\lambda_d\sigma)\,d\sigma \quad \text{(I-2)}$$

Let

$$\gamma=\frac{1}{\sqrt{\sigma-\zeta_0}} \qquad \sigma=\zeta_0+\frac{1}{\gamma^2} \qquad d\gamma=-\frac{1}{2}\frac{d\mu}{(\sigma-\zeta_0)^{\frac{3}{2}}}$$

$$\sigma=\zeta_0 \quad \Rightarrow \quad \gamma\to\infty$$

$$\sigma=\psi \quad \Rightarrow \quad \gamma=\frac{1}{\sqrt{\psi-\zeta_0}}$$

Substituting for σ in Equation (I-2) gives,

$$\frac{M_f}{M_0}(\psi)=\int_{\frac{1}{\sqrt{\psi-\zeta_0}}}^{\infty}\frac{\zeta_0-V_\ell\left(\zeta_0+\frac{1}{\gamma^2}\right)}{\sqrt{\pi}\sqrt{Pe}}\exp\left[-\left\{\frac{\frac{PeV}{\gamma^2}+\zeta_0-V_\ell\left(\zeta_0+\frac{1}{\gamma^2}\right)}{\frac{2\sqrt{Pe}}{\gamma}}\right\}^2\right]\bullet \quad \text{(I-3)}$$

$$\exp\left\{-\lambda_d\left(\zeta_0+\frac{1}{\gamma^2}\right)\right\}d\gamma$$

rearranging terms in Equation (I-3) gives

$$\frac{M_f}{M_0}(\psi) = \int_{\frac{1}{\sqrt{\psi-\zeta_0}}}^{\infty} \left(\frac{\zeta_0\{1-V_\ell\}}{\sqrt{\pi}\sqrt{Pe}} - \frac{V_\ell}{\sqrt{\pi}\sqrt{Pe}\gamma^2} \right) \bullet$$

$$\exp\left[-\left\{ \frac{\frac{PeV}{\gamma} + \zeta_0\gamma - V_\ell\zeta_0\gamma - \frac{V_\ell}{\gamma}}{2\sqrt{Pe}} \right\}^2 - \lambda_d\left(\zeta_0 + \frac{1}{\gamma^2} \right) \right] d\gamma \qquad \text{(I-4)}$$

or

$$\frac{M_f}{M_0}(\psi) = \int_{\frac{1}{\sqrt{\psi-\zeta_0}}}^{\infty} \left(\frac{\zeta_0\{1-V_\ell\}}{\sqrt{\pi}\sqrt{Pe}} - \frac{V_\ell}{\sqrt{\pi}\sqrt{Pe}\gamma^2} \right) \bullet$$

$$\exp\left[-\left\{ \frac{\zeta_0(1-V_\ell)\gamma + (PeV - V_\ell)\frac{1}{\gamma}}{2\sqrt{Pe}} \right\}^2 - \lambda_d\left(\zeta_0 + \frac{1}{\gamma^2} \right) \right] d\gamma \qquad \text{(I-5)}$$

Expanding the square in the exponential term gives,

$$\left\{ \zeta_0(1-V_\ell)\gamma + (PeV - V_\ell)\frac{1}{\gamma} \right\}^2 = \zeta_0^2(1-V_\ell)^2\gamma^2 + 2\zeta_0(1-V_\ell)(PeV - V_\ell) + (PeV - V_\ell)^2\frac{1}{\gamma^2} \qquad \text{(I-6)}$$

Substituting Equation (I-6) into Equation (I-5) gives,

$$\frac{M_f}{M_0}(\psi) = \int_{\frac{1}{\sqrt{\psi-\zeta_0}}}^{\infty} \left\{ \frac{\zeta_0(1-V_\ell)}{\sqrt{\pi}\sqrt{Pe}} - \frac{V_\ell}{\sqrt{\pi}\sqrt{Pe}}\frac{1}{\gamma^2} \right\} \exp\left[\frac{-\zeta_0}{2Pe}\{(1-V_\ell)(PeV - V_\ell) + 2Pe\lambda_d\} \right] \bullet$$

$$\exp\left[-\left\{ \frac{\zeta_0(1-V_\ell)}{2\sqrt{Pe}} \right\}^2 \gamma^2 - \left\{ \left(\frac{PeV - V_\ell}{2\sqrt{Pe}} \right)^2 + \lambda_d \right\} \frac{1}{\gamma^2} \right] d\gamma \qquad \text{(I-7)}$$

Rearranging terms gives,

$$\frac{M_f}{M_0}(\psi) = \frac{\zeta_0(1-V_\ell)}{\sqrt{\pi}\sqrt{Pe}} \exp\left[-\frac{\zeta_0}{2Pe}\{(1-V_\ell)(PeV-V_\ell)+2Pe\lambda_d\}\right] \bullet$$
$$\int_{\frac{1}{\sqrt{\psi-\zeta_0}}}^{\infty} \exp\left[-\left\{\frac{\zeta_0(1-V_\ell)}{2\sqrt{Pe}}\right\}^2 \gamma^2 - \left\{\left(\frac{PeV-V_\ell}{2\sqrt{Pe}}\right)^2 + \lambda_d\right\}\frac{1}{\gamma^2}\right] d\gamma$$
$$-\frac{V_\ell}{\sqrt{\pi}\sqrt{Pe}} \exp\left[-\frac{\zeta_0}{2Pe}\{(1-V_\ell)(PeV-V_\ell)+2Pe\lambda_d\}\right] \bullet \qquad \text{(I-8)}$$
$$\int_{\frac{1}{\sqrt{\psi-\zeta_0}}}^{\infty} \frac{1}{\gamma^2} \exp\left[-\left\{\frac{\zeta_0(1-V_\ell)}{2\sqrt{Pe}}\right\}^2 \gamma^2 - \left\{\left(\frac{PeV-V_\ell}{2\sqrt{Pe}}\right)^2 + \lambda_d\right\}\frac{1}{\gamma^2}\right] d\gamma$$

For the second integral in Equation (I-8), let

$$\omega = \frac{1}{\gamma} \quad d\omega = -\frac{1}{\gamma^2} d\gamma$$
$$\gamma \to \infty \quad \Rightarrow \quad \omega = 0$$
$$\gamma = \frac{1}{\sqrt{\psi-\zeta_0}} \quad \Rightarrow \quad \omega = \sqrt{\psi-\zeta_0}$$

Substituting for γ in the second integral gives,

$$\frac{M_f}{M_0}(\psi) = \frac{\zeta_0(1-V_\ell)}{\sqrt{\pi}\sqrt{Pe}} \exp\left[-\frac{\zeta_0}{2Pe}\{(1-V_\ell)(PeV-V_\ell)+2Pe\lambda_d\}\right] \bullet$$
$$\int_{\frac{1}{\sqrt{\psi-\zeta_0}}}^{\infty} \exp\left[-\left\{\frac{\zeta_0(1-V_\ell)}{2\sqrt{Pe}}\right\}^2 \gamma^2 - \left\{\left(\frac{PeV-V_\ell}{2\sqrt{Pe}}\right)^2 + \lambda_d\right\}\frac{1}{\gamma^2}\right] d\gamma$$
$$-\frac{V_\ell}{\sqrt{\pi}\sqrt{Pe}} \exp\left[-\frac{\zeta_0}{2Pe}\{(1-V_\ell)(PeV-V_\ell)+2Pe\lambda_d\}\right] \bullet \qquad \text{(I-9)}$$
$$\int_0^{\sqrt{\psi-\zeta_0}} \exp\left[-\left\{\left(\frac{PeV-V_\ell}{2\sqrt{Pe}}\right)^2 + \lambda_d\right\}\omega^2 - \left\{\frac{\zeta_0(1-V_\ell)}{2\sqrt{Pe}}\right\}^2 \frac{1}{\omega^2}\right] d\omega$$

In general,

$$\int e^{-a^2x^2-\frac{b^2}{x^2}} dx = \frac{\sqrt{\pi}}{4a}\left[e^{2ab}\,\mathrm{erf}\left(ax+\frac{b}{x}\right) + e^{-2ab}\,\mathrm{erf}\left(ax-\frac{b}{x}\right)\right] + C \qquad \text{(I-10)}$$

where *C* is a constant.

Expressing the integrals in Equation (I-9) in this general form gives,

$$\frac{M_f}{M_0}(\psi) = \frac{\zeta_0(1-V_\ell)}{\sqrt{\pi}\sqrt{Pe}}\exp(-A)\int_{\frac{1}{\sqrt{\psi-\zeta_0}}}^{\infty}\exp\left(-a^2\gamma^2-\frac{b^2}{\gamma^2}\right)d\gamma$$
$$-\frac{V_\ell}{\sqrt{\pi}\sqrt{Pe}}\exp(-A)\int_0^{\sqrt{\psi-\zeta_0}}\exp\left(-a'^2\omega^2-\frac{b'^2}{\omega^2}\right)d\omega \qquad \text{(I-11)}$$

where

$$a=\frac{\zeta_0(1-V_\ell)}{2\sqrt{Pe}} \qquad b=\left\{\left(\frac{PeV-V_\ell}{2\sqrt{Pe}}\right)^2+\lambda_d\right\}^{\frac{1}{2}} \qquad A=\frac{\zeta_0}{2Pe}\left\{(1-V_\ell)(PeV-V_\ell)+2Pe\lambda_d\right\}$$

$$a'=\left\{\left(\frac{PeV-V_\ell}{2\sqrt{Pe}}\right)^2+\lambda_d\right\}^{\frac{1}{2}} \qquad b'=\frac{\zeta_0(1-V_\ell)}{2\sqrt{Pe}}$$

Using the general result in Equation (I-10) to evaluate the integrals in Equation (I-11) gives,

$$\frac{M_f}{M_0}(\psi) = \frac{\zeta_0(1-V_\ell)}{\sqrt{\pi}\sqrt{Pe}}\frac{\sqrt{\pi}}{4\frac{\zeta_0(1-V_\ell)}{2\sqrt{Pe}}}\bullet$$
$$\left[\begin{array}{l}\exp(-A-2ab)+\exp(-A+2ab)\\ -\exp(-A-2ab)\operatorname{erf}\left(\frac{a}{\sqrt{\psi-\zeta}}-b\sqrt{\psi-\zeta}\right)\\ -\exp(-A+2ab)\operatorname{erf}\left(\frac{a}{\sqrt{\psi-\zeta}}+b\sqrt{\psi-\zeta}\right)\end{array}\right]$$
$$-\frac{V_\ell}{\sqrt{\pi}\sqrt{Pe}}\frac{\sqrt{\pi}}{4\left\{\left(\frac{PeV-V_\ell}{2\sqrt{Pe}}\right)^2+\lambda_d\right\}^{\frac{1}{2}}}\bullet$$
$$\left[\begin{array}{l}\exp(-A-2ab)\operatorname{erf}\left(a'\sqrt{\psi-\zeta}-\frac{b'}{\sqrt{\psi-\zeta}}\right)\\ +\exp(-A+2ab)\operatorname{erf}\left(a'\sqrt{\psi-\zeta}+\frac{b'}{\sqrt{\psi-\zeta}}\right)\\ +\exp(-A-2ab)-\exp(-A+2ab)\end{array}\right] \qquad \text{(I-12)}$$

Rearranging, and using the definition of the complementary error function, Equation (I-12) becomes,

$$\frac{M_f}{M_0}(\psi) = \frac{1}{2}\left[\begin{array}{l} \exp(-A+2ab)\operatorname{erfc}\left(\dfrac{a}{\sqrt{\psi-\zeta}}+b\sqrt{\psi-\zeta}\right) \\ +\exp(-A-2ab)\operatorname{erfc}\left(\dfrac{a}{\sqrt{\psi-\zeta}}-b\sqrt{\psi-\zeta}\right) \end{array}\right] \qquad \text{(I-13)}$$

$$-\frac{V_\ell}{4\sqrt{Pe}\left\{\left(\dfrac{PeV-V_\ell}{2\sqrt{Pe}}\right)^2+\lambda_d\right\}^{\frac{1}{2}}}\left[\begin{array}{l} -\exp(-A+2ab)\operatorname{erfc}\left(a'\sqrt{\psi-\zeta}+\dfrac{b'}{\sqrt{\psi-\zeta}}\right) \\ +\exp(-A-2ab)\operatorname{erfc}\left(\dfrac{b'}{\sqrt{\psi-\zeta}}-a'\sqrt{\psi-\zeta}\right) \end{array}\right]$$

Substituting for A, a, b, a', and b' in Equation (I-13) gives,

$$\frac{M_f}{M_0}(\psi)=\frac{1}{2}\left[\begin{array}{l}\exp\left[-\frac{\zeta_0}{2Pe}\left\{(1-V_\ell)(PeV-V_\ell)+2Pe\lambda_d\right\}+\frac{\zeta_0(1-V_\ell)}{\sqrt{Pe}}\left\{\left(\frac{PeV-V_\ell}{2\sqrt{Pe}}\right)^2+\lambda_d\right\}^{\frac{1}{2}}\right]\\ \bullet\ \mathrm{erfc}\left\{\frac{\zeta_0(1-V_\ell)}{2\sqrt{Pe}\sqrt{\psi-\zeta_0}}+\left\{\left(\frac{PeV-V_\ell}{2\sqrt{Pe}}\right)^2+\lambda_d\right\}^{\frac{1}{2}}\sqrt{\psi-\zeta_0}\right\}\\ +\exp\left[-\frac{\zeta_0}{2Pe}\left\{(1-V_\ell)(PeV-V_\ell)+2Pe\lambda_d\right\}-\frac{\zeta_0(1-V_\ell)}{\sqrt{Pe}}\left\{\left(\frac{PeV-V_\ell}{2\sqrt{Pe}}\right)^2+\lambda_d\right\}^{\frac{1}{2}}\right]\\ \bullet\ \mathrm{erfc}\left\{\frac{\zeta_0(1-V_\ell)}{2\sqrt{Pe}\sqrt{\psi-\zeta_0}}-\left\{\left(\frac{PeV-V_\ell}{2\sqrt{Pe}}\right)^2+\lambda_d\right\}^{\frac{1}{2}}\sqrt{\psi-\zeta_0}\right\}\end{array}\right]$$

$$+\frac{V_\ell}{4\sqrt{Pe}\left\{\left(\frac{PeV-V_\ell}{2\sqrt{Pe}}\right)^2+\lambda_d\right\}^{\frac{1}{2}}}$$

$$\bullet\left[\begin{array}{l}\exp\left[-\frac{\zeta_0}{2Pe}\left\{(1-V_\ell)(PeV-V_\ell)+2Pe\lambda_d\right\}+\frac{\zeta_0(1-V_\ell)}{\sqrt{Pe}}\left\{\left(\frac{PeV-V_\ell}{2\sqrt{Pe}}\right)^2+\lambda_d\right\}^{\frac{1}{2}}\right]\\ \bullet\ \mathrm{erfc}\left\{\frac{\zeta_0(1-V_\ell)}{2\sqrt{Pe}\sqrt{\psi-\zeta_0}}+\left\{\left(\frac{PeV-V_\ell}{2\sqrt{Pe}}\right)^2+\lambda_d\right\}^{\frac{1}{2}}\sqrt{\psi-\zeta_0}\right\}\\ -\exp\left[-\frac{\zeta_0}{2Pe}\left\{(1-V_\ell)(PeV-V_\ell)+2Pe\lambda_d\right\}-\frac{\zeta_0(1-V_\ell)}{\sqrt{Pe}}\left\{\left(\frac{PeV-V_\ell}{2\sqrt{Pe}}\right)^2+\lambda_d\right\}^{\frac{1}{2}}\right]\\ \bullet\ \mathrm{erfc}\left\{\frac{\zeta_0(1-V_\ell)}{2\sqrt{Pe}\sqrt{\psi-\zeta_0}}-\left\{\left(\frac{PeV-V_\ell}{2\sqrt{Pe}}\right)^2+\lambda_d\right\}^{\frac{1}{2}}\sqrt{\psi-\zeta_0}\right\}\end{array}\right] \qquad \text{(I-14)}$$

Note that

$$\frac{1}{2}+\frac{V_\ell}{4\sqrt{Pe}\left\{\left(\frac{PeV-V_\ell}{2\sqrt{Pe}}\right)^2+\lambda_d\right\}^{\frac{1}{2}}}=\frac{2\sqrt{Pe}\left\{\left(\frac{PeV-V_\ell}{2\sqrt{Pe}}\right)^2+\lambda_d\right\}^{\frac{1}{2}}+V_\ell}{4\sqrt{Pe}\left\{\left(\frac{PeV-V_\ell}{2\sqrt{Pe}}\right)^2+\lambda_d\right\}^{\frac{1}{2}}} \tag{I-15}$$

$$\frac{1}{2}-\frac{V_\ell}{4\sqrt{Pe}\left\{\left(\frac{PeV-V_\ell}{2\sqrt{Pe}}\right)^2+\lambda_d\right\}^{\frac{1}{2}}}=\frac{2\sqrt{Pe}\left\{\left(\frac{PeV-V_\ell}{2\sqrt{Pe}}\right)^2+\lambda_d\right\}^{\frac{1}{2}}-V_\ell}{4\sqrt{Pe}\left\{\left(\frac{PeV-V_\ell}{2\sqrt{Pe}}\right)^2+\lambda_d\right\}^{\frac{1}{2}}} \tag{I-16}$$

Using Equations (I-15) and (I-16) in Equation (I-14) gives,

$$\frac{M_f}{M_0}(\psi) = \frac{2\sqrt{Pe}\left\{\left(\frac{PeV - V_\ell}{2\sqrt{Pe}}\right)^2 + \lambda_d\right\}^{\frac{1}{2}} + V_\ell}{4\sqrt{Pe}\left\{\left(\frac{PeV - V_\ell}{2\sqrt{Pe}}\right)^2 + \lambda_d\right\}^{\frac{1}{2}}} \bullet$$

$$\exp\left[-\frac{\zeta_0}{2Pe}\left\{(1-V_\ell)(PeV - V_\ell) + 2Pe\lambda_d\right\} + \frac{\zeta_0(1-V_\ell)}{\sqrt{Pe}}\left\{\left(\frac{PeV - V_\ell}{2\sqrt{Pe}}\right)^2 + \lambda_d\right\}^{\frac{1}{2}}\right] \bullet$$

$$\operatorname{erfc}\left\{\frac{\zeta_0(1-V_\ell)}{2\sqrt{Pe}\sqrt{\psi - \zeta_0}} + \left\{\left(\frac{PeV - V_\ell}{2\sqrt{Pe}}\right)^2 + \lambda_d\right\}^{\frac{1}{2}}\sqrt{\psi - \zeta_0}\right\}$$

$$+ \frac{2\sqrt{Pe}\left\{\left(\frac{PeV - V_\ell}{2\sqrt{Pe}}\right)^2 + \lambda_d\right\}^{\frac{1}{2}} - V_\ell}{4\sqrt{Pe}\left\{\left(\frac{PeV - V_\ell}{2\sqrt{Pe}}\right)^2 + \lambda_d\right\}^{\frac{1}{2}}} \bullet$$

$$\exp\left[-\frac{\zeta_0}{2Pe}\left\{(1-V_\ell)(PeV - V_\ell) + 2Pe\lambda_d\right\} - \frac{\zeta_0(1-V_\ell)}{\sqrt{Pe}}\left\{\left(\frac{PeV - V_\ell}{2\sqrt{Pe}}\right)^2 + \lambda_d\right\}^{\frac{1}{2}}\right] \bullet$$

$$\operatorname{erfc}\left\{\frac{\zeta_0(1-V_\ell)}{2\sqrt{Pe}\sqrt{\psi - \zeta_0}} - \left\{\left(\frac{PeV - V_\ell}{2\sqrt{Pe}}\right)^2 + \lambda_d\right\}^{\frac{1}{2}}\sqrt{\psi - \zeta_0}\right\} \qquad \text{(I-17)}$$

Simplifying equation (I-17) gives,

$$\frac{M_f}{M_0}(\psi) = \frac{\left\{(PeV - V_\ell)^2 + 4Pe\lambda_d\right\}^{\frac{1}{2}} + V_\ell}{2\left\{(PeV - V_\ell)^2 + 4Pe\lambda_d\right\}^{\frac{1}{2}}} \bullet$$

$$\exp\left[-\frac{\zeta_0}{2Pe}\left\{(1-V_\ell)(PeV - V_\ell) + 2Pe\lambda_d\right\} + \frac{\zeta_0(1-V_\ell)}{2Pe}\left\{(PeV - V_\ell)^2 + 4Pe\lambda_d\right\}^{\frac{1}{2}}\right] \bullet$$

$$\operatorname{erfc}\left\{\frac{\left\{(PeV - V_\ell)^2 + 4Pe\lambda_d\right\}^{\frac{1}{2}}(\psi - \zeta_0) + \zeta_0(1-V_\ell)}{2\sqrt{Pe}\sqrt{\psi - \zeta_0}}\right\}$$

$$- \frac{\left\{(PeV - V_\ell)^2 + 4Pe\lambda_d\right\}^{\frac{1}{2}} - V_\ell}{2\left\{(PeV - V_\ell)^2 + 4Pe\lambda_d\right\}^{\frac{1}{2}}} \bullet$$

$$\exp\left[-\frac{\zeta_0}{2Pe}\left\{(1-V_\ell)(PeV - V_\ell) + 2Pe\lambda_d\right\} - \frac{\zeta_0(1-V_\ell)}{2Pe}\left\{(PeV - V_\ell)^2 + 4Pe\lambda_d\right\}^{\frac{1}{2}}\right] \bullet$$

$$\operatorname{erfc}\left\{\frac{\left\{(PeV - V_\ell)^2 + 4Pe\lambda_d\right\}^{\frac{1}{2}}(\psi - \zeta_0) - \zeta_0(1-V_\ell)}{2\sqrt{Pe}\sqrt{\psi - \zeta_0}}\right\} \tag{I-18}$$

Further simplification of equation (I-18) gives Equation (66) of the main text,

$$\frac{M_f}{M_0}(\psi) = \frac{\exp\left[-\frac{\zeta_0}{2Pe}\left\{(1-V_\ell)(PeV-V_\ell)+2Pe\lambda_d\right\}\right]}{2\left\{(PeV-V_\ell)^2+4Pe\lambda_d\right\}^{\frac{1}{2}}} \bullet$$

$$\left[\begin{array}{l}
\left\{\left\{(PeV-V_\ell)^2+4Pe\lambda_d\right\}^{\frac{1}{2}}+V_\ell\right\}\bullet \\
\exp\left[\frac{\zeta_0(1-V_\ell)}{2Pe}\left\{(PeV-V_\ell)^2+4Pe\lambda_d\right\}^{\frac{1}{2}}\right]\bullet \\
\quad \operatorname{erfc}\left\{\frac{\left\{(PeV-V_\ell)^2+4Pe\lambda_d\right\}^{\frac{1}{2}}(\psi-\zeta_0)+\zeta_0(1-V_\ell)}{2\sqrt{Pe}\sqrt{\psi-\zeta_0}}\right\} \\
-\left\{\left\{(PeV-V_\ell)^2+4Pe\lambda_d\right\}^{\frac{1}{2}}-V_\ell\right\}\bullet \\
\exp\left[-\frac{\zeta_0(1-V_\ell)}{2Pe}\left\{(PeV-V_\ell)^2+4Pe\lambda_d\right\}^{\frac{1}{2}}\right]\bullet \\
\quad \operatorname{erfc}\left\{\frac{\left\{(PeV-V_\ell)^2+4Pe\lambda_d\right\}^{\frac{1}{2}}(\psi-\zeta_0)-\zeta_0(1-V_\ell)}{2\sqrt{Pe}\sqrt{\psi-\zeta_0}}\right\}
\end{array}\right] \qquad \text{(I-19)}$$

for $\zeta_0 \le \psi \le \frac{\zeta_0}{V_\ell}$,

for $\psi < \zeta_0$, $\frac{M_f}{M_0}(\psi) = 0$,

for $\frac{\zeta_0}{V_\ell} < \psi$, the solution has achieved steady-state and $\frac{M_f}{M_0}(\psi) = \frac{M_f}{M_0}\left(\frac{\zeta_0}{V_\ell}\right)$.

Appendix II – Derivation of the Solution for the Laplace Transformed Matrix and Fracture Concentrations from an Instantaneous, Point Source in the Matrix

As for the fracture source case, solve Equation (34) using the Laplace transform. Substitute for c_{md} using the Laplace transform:

$$c_{md}(\eta,\xi,\tau) = \frac{1}{2\pi i}\int_{c-i\infty}^{c+i\infty} \hat{c}_{md}(\eta,\xi,s)e^{s\tau}\,ds \tag{II-1}$$

which leads to the following ordinary differential equation:

$$\frac{d^2\hat{c}_{md}}{d\eta^2} - Pe\,V\frac{d\hat{c}_{md}}{d\eta} - s\,Pe\,\hat{c}_{md} = -Pe\,\delta(\eta-\eta_0)\delta(\xi) \tag{II-2}$$

The general solution, $\hat{c}^-_{md}(\eta,\xi,s)$, for $\eta<\eta_0$ is,

$$\hat{c}^-_{md}(\eta,\xi,s) = A(\xi,s)\exp\left[\left(\frac{PeV}{2}+\sqrt{\left(\frac{PeV}{2}\right)^2+sPe}\right)\eta\right] + B(\xi,s)\exp\left[\left(\frac{PeV}{2}-\sqrt{\left(\frac{PeV}{2}\right)^2+sPe}\right)\eta\right] \tag{II-3}$$

and the general solution, $\hat{c}^+_{md}(\eta,\xi,s)$, for $\eta>\eta_0$ is,

$$\hat{c}^+_{md}(\eta,\xi,s) = C(\xi,s)\exp\left[\left(\frac{PeV}{2}+\sqrt{\left(\frac{PeV}{2}\right)^2+sPe}\right)\eta\right] + D(\xi,s)\exp\left[\left(\frac{PeV}{2}-\sqrt{\left(\frac{PeV}{2}\right)^2+sPe}\right)\eta\right] \tag{II-4}$$

Boundary and continuity conditions:

$$\hat{c}^-_{md}(0,\xi,s) = \hat{c}_{fd}(\xi,s) \tag{II-5}$$

$$\lim_{\eta\to\infty}\hat{c}^+_{md}(\eta,\xi,s) = 0 \tag{II-6}$$

$$\hat{c}^-_{md}(\eta_0,\xi,s) = \hat{c}^+_{m}(\eta_0,\xi,s) \tag{II-7}$$

and integrating Equation (II-2) from $\eta-\varepsilon$ to $\eta+\varepsilon$, $\lim_{\varepsilon\to 0}$ gives,

$$\left[\frac{d\hat{c}^-_{md}}{d\eta}\right]_{\eta_0} - \left[\frac{d\hat{c}^+_{md}}{d\eta}\right]_{\eta_0} = Pe\,\delta(\xi) \tag{II-8}$$

Equation (II-6) implies $C(\xi,s)=0$.

Using Equation (II-5) in Equation (II-3) gives,

$$A(\xi,s)+B(\xi,s)=\hat{c}_{fd}(\xi,s) \tag{II-9}$$

Using Equation (II-7) with Equations (II-3) and (II-4) gives,

$$\begin{aligned}
&A(\xi,s)\exp\left[\left(\frac{PeV}{2}+\sqrt{\left(\frac{PeV}{2}\right)^2+sPe}\right)\eta_0\right] \\
&+B(\xi,s)\exp\left[\left(\frac{PeV}{2}-\sqrt{\left(\frac{PeV}{2}\right)^2+sPe}\right)\eta_0\right] \\
&=D(\xi,s)\exp\left[\left(\frac{PeV}{2}-\sqrt{\left(\frac{PeV}{2}\right)^2+sPe}\right)\eta_0\right]
\end{aligned} \tag{II-10}$$

and using Equation (II-8) with Equations (II-3) and (II-4) gives,

$$\begin{aligned}
&A(\xi,s)\left(\frac{PeV}{2}+\sqrt{\left(\frac{PeV}{2}\right)^2+sPe}\right)\exp\left[\left(\frac{PeV}{2}+\sqrt{\left(\frac{PeV}{2}\right)^2+sPe}\right)\eta_0\right] \\
&+B(\xi,s)\left(\frac{PeV}{2}-\sqrt{\left(\frac{PeV}{2}\right)^2+sPe}\right)\exp\left[\left(\frac{PeV}{2}-\sqrt{\left(\frac{PeV}{2}\right)^2+sPe}\right)\eta_0\right] \\
&-D(\xi,s)\left(\frac{PeV}{2}-\sqrt{\left(\frac{PeV}{2}\right)^2+sPe}\right)\exp\left[\left(\frac{PeV}{2}-\sqrt{\left(\frac{PeV}{2}\right)^2+sPe}\right)\eta_0\right]=Pe\delta(\xi)
\end{aligned} \tag{II-11}$$

Let

$$\gamma^+=\frac{PeV}{2}+\sqrt{\left(\frac{PeV}{2}\right)^2+sPe}$$

$$\gamma-=\frac{PeV}{2}-\sqrt{\left(\frac{PeV}{2}\right)^2+sPe}$$

Then from Equations (II-9), (II-10), and (II-11)

$$A+B=\hat{c}_{fd} \tag{II-12}$$

$$Ae^{\gamma^+\eta_0}+Be^{\gamma^-\eta_0}=De^{\gamma^-\eta_0} \tag{II-13}$$

$$A\gamma^+e^{\gamma^+\eta_0}+B\gamma^-e^{\gamma^-\eta_0}=D\gamma^-e^{\gamma^-\eta_0}+Pe\delta(\xi) \tag{II-14}$$

Use equation (II-12) to solve for *B* and substitute into equations (II-13) and (II-14) to give,

$$A\left(e^{\gamma^+\eta_0}-e^{\gamma^-\eta_0}\right)+\hat{c}_{fd}e^{\gamma^-\eta_0}=De^{\gamma^-\eta_0} \tag{II-15}$$

$$\text{Note}: D = \hat{c}_{fd} - A + Ae^{(\gamma^+ - \gamma^-)\eta_0} \tag{II-16}$$

$$A\left(\gamma^+ e^{\gamma^+\eta_0} - \gamma^- e^{\gamma^-\eta_0}\right) + \hat{c}_{fd}\gamma^- e^{\gamma^-\eta_0} = D\gamma^- e^{\gamma^-\eta_0} + Pe\delta \tag{II-17}$$

Eliminate *D;* multiply equation (II-15) by $-\gamma^-$ and add to equation (II-17) to give,

$$\begin{aligned} &A\left(\gamma^+ e^{\gamma^+\eta_0} - \gamma^- e^{\gamma^-\eta_0} - \gamma^- e^{\gamma^+\eta_0} + \gamma^- e^{\gamma^-\eta_0}\right) + \hat{c}_{fd}\left(\gamma^- e^{\gamma^-\eta_0} - \gamma^- e^{\gamma^-\eta_0}\right) \\ &= D\left(\gamma^- e^{\gamma^-\eta_0} - \gamma^- e^{\gamma^-\eta_0}\right) + Pe\delta \end{aligned} \tag{II-18}$$

Simplifying equation (II-18) gives,

$$A\left(\gamma^+ - \gamma^-\right)e^{\gamma^+\eta_0} = Pe\delta \tag{II-19}$$

or

$$A = \frac{Pe\delta\, e^{-\gamma^+\eta_0}}{\left(\gamma^+ - \gamma^-\right)} \tag{II-20}$$

Using equations (II-12) and (II-20), solve for *B*,

$$B = \hat{c}_{fd} - \frac{Pe\delta\, e^{-\gamma^+\eta_0}}{\left(\gamma^+ - \gamma^-\right)} \tag{II-21}$$

and using equations (II-16) and (II-20), solve for *D*,

$$D = \hat{c}_{fd} - \frac{Pe\delta\, e^{-\gamma^+\eta_0}}{\left(\gamma^+ - \gamma^-\right)} + \frac{Pe\delta\, e^{-\gamma^-\eta_0}}{\left(\gamma^+ - \gamma^-\right)} \tag{II-22}$$

Now,

$$\gamma^+ - \gamma^- = 2\sqrt{\left(\frac{PeV}{2}\right)^2 + sPe}$$

Therefore, $A(\xi, s), B(\xi, s), \text{and } D(\xi, s)$ become,

$$A(\xi, s) = \frac{Pe\delta(\xi)\exp\left[-\left\{\frac{PeV}{2} + \sqrt{\left(\frac{PeV}{2}\right)^2 + sPe}\right\}\eta_0\right]}{2\sqrt{\left(\frac{PeV}{2}\right)^2 + sPe}} \tag{II-23}$$

$$B(\xi,s)=\hat{c}_{fd}(\xi,s)-\frac{Pe\delta(\xi)\exp\left[-\left\{\frac{PeV}{2}+\sqrt{\left(\frac{PeV}{2}\right)^2+sPe}\right\}\eta_0\right]}{2\sqrt{\left(\frac{PeV}{2}\right)^2+sPe}} \tag{II-24}$$

$$\begin{aligned}D(\xi,s)=\hat{c}_{fd}(\xi,s)&+\frac{Pe\delta(\xi)\exp\left[-\left\{\frac{PeV}{2}-\sqrt{\left(\frac{PeV}{2}\right)^2+sPe}\right\}\eta_0\right]}{2\sqrt{\left(\frac{PeV}{2}\right)^2+sPe}}\\&-\frac{Pe\delta(\xi)\exp\left[-\left\{\frac{PeV}{2}+\sqrt{\left(\frac{PeV}{2}\right)^2+sPe}\right\}\eta_0\right]}{2\sqrt{\left(\frac{PeV}{2}\right)^2+sPe}}\end{aligned} \tag{II-25}$$

Using Equations (II-23) and (II-24) in Equation (II-3) gives (for $\eta<\eta_0$),

$$\begin{aligned}\hat{c}^{-}_{md}(\eta,\xi,s)=\hat{c}_{fd}(\xi,s)&\exp\left[\left\{\frac{PeV}{2}-\sqrt{\left(\frac{PeV}{2}\right)^2+sPe}\right\}\eta\right]\\&+\frac{Pe\delta(\xi)\exp\left[\left(\frac{PeV}{2}+\sqrt{\left(\frac{PeV}{2}\right)^2+sPe}\right)(\eta-\eta_0)\right]}{2\sqrt{\left(\frac{PeV}{2}\right)^2+sPe}}\\&-\frac{Pe\delta(\xi)\exp\left[\frac{PeV}{2}(\eta-\eta_0)-\left(\sqrt{\left(\frac{PeV}{2}\right)^2+sPe}\right)(\eta+\eta_0)\right]}{2\sqrt{\left(\frac{PeV}{2}\right)^2+sPe}}\end{aligned} \tag{II-26}$$

Using Equation (II-25) in Equation (II-4) and noting that $C(\xi,s)=0$ gives (for $\eta>\eta_0$),

$$\hat{c}^{+}_{md}(\eta,\xi,s)=\hat{c}_{fd}(\xi,s)\exp\left[\left\{\frac{PeV}{2}-\sqrt{\left(\frac{PeV}{2}\right)^2+sPe}\right\}\eta\right]$$
$$+\frac{Pe\delta(\xi)\exp\left[\left(\frac{PeV}{2}-\sqrt{\left(\frac{PeV}{2}\right)^2+sPe}\right)(\eta-\eta_0)\right]}{2\sqrt{\left(\frac{PeV}{2}\right)^2+sPe}} \qquad \text{(II-27)}$$
$$-\frac{Pe\delta(\xi)\exp\left[\frac{PeV}{2}(\eta-\eta_0)-\left(\sqrt{\left(\frac{PeV}{2}\right)^2+sPe}\right)(\eta+\eta_0)\right]}{2\sqrt{\left(\frac{PeV}{2}\right)^2+sPe}}$$

Equations (II-26) and (II-27) are the results presented in Equations (86) and (87) of the main text.

To solve Equation (29) for the fracture concentration, use the Laplace transform for the fracture and matrix concentrations given in Equations (38) and (39), which leads to the following ordinary differential equation,

$$\frac{d\hat{c}_{fd}}{d\xi}+s\hat{c}_{fd}=\frac{1}{Pe}\frac{d\hat{c}_{md}}{d\eta}\bigg|_{\eta=0}-V\hat{c}_{md}\big|_{\eta=0} \qquad \text{(II-28)}$$

Evaluate the derivative of $\hat{c}^{-}_{md}$ using Equation (iV-26),

$$\frac{d\hat{c}^{-}_{md}}{d\eta}=\left\{\frac{PeV}{2}-\sqrt{\left(\frac{PeV}{2}\right)^2+sPe}\right\}\hat{c}_{fd}\exp\left[\left(\frac{PeV}{2}-\sqrt{\left(\frac{PeV}{2}\right)^2+sPe}\right)\eta\right]$$
$$+\frac{1}{2\sqrt{\left(\frac{PeV}{2}\right)^2+sPe}}\left[\begin{array}{l}Pe\delta(\xi)\left\{\frac{PeV}{2}+\sqrt{\left(\frac{PeV}{2}\right)^2+sPe}\right\}\bullet \\ \exp\left[\left(\frac{PeV}{2}+\sqrt{\left(\frac{PeV}{2}\right)^2+sPe}\right)(\eta-\eta_0)\right]\end{array}\right]$$
$$-\frac{1}{2\sqrt{\left(\frac{PeV}{2}\right)^2+sPe}}\left[\begin{array}{l}Pe\delta(\xi)\left\{\frac{PeV}{2}-\sqrt{\left(\frac{PeV}{2}\right)^2+sPe}\right\}\bullet \\ \exp\left[\frac{PeV}{2}(\eta-\eta_0)-\left\{\sqrt{\left(\frac{PeV}{2}\right)^2+sPe}\right\}(\eta+\eta_0)\right]\end{array}\right] \qquad \text{(II-29)}$$

Evaluating equation (iV-29) at $\eta = 0$ gives,

$$\left.\frac{d\hat{c}_{md}^{-}}{d\eta}\right|_{\eta=0} = \left\{\frac{PeV}{2} - \sqrt{\left(\frac{PeV}{2}\right)^2 + sPe}\right\}\hat{c}_{fd} + \frac{1}{2\sqrt{\left(\frac{PeV}{2}\right)^2 + sPe}}\left[\begin{array}{l} Pe\delta(\xi)\left\{\frac{PeV}{2} + \sqrt{\left(\frac{PeV}{2}\right)^2 + sPe}\right\}\bullet \\ \exp\left[-\left(\frac{PeV}{2} + \sqrt{\left(\frac{PeV}{2}\right)^2 + sPe}\right)\eta_0\right]\end{array}\right] - \frac{1}{2\sqrt{\left(\frac{PeV}{2}\right)^2 + sPe}}\left[\begin{array}{l} Pe\delta(\xi)\left\{\frac{PeV}{2} - \sqrt{\left(\frac{PeV}{2}\right)^2 + sPe}\right\}\bullet \\ \exp\left[-\left(\frac{PeV}{2} + \left\{\sqrt{\left(\frac{PeV}{2}\right)^2 + sPe}\right\}\right)\eta_0\right]\end{array}\right] \quad \text{(II-30)}$$

Simplifying Equation (II-30) gives,

$$\left.\frac{d\hat{c}_{md}^{-}}{d\eta}\right|_{\eta=0} = \left\{\frac{PeV}{2} - \sqrt{\left(\frac{PeV}{2}\right)^2 + sPe}\right\}\hat{c}_{fd} + Pe\delta(\xi)\exp\left[-\left(\frac{PeV}{2} + \sqrt{\left(\frac{PeV}{2}\right)^2 + sPe}\right)\eta_0\right] \quad \text{(II-31)}$$

Therefore,

$$\frac{1}{Pe}\left.\frac{d\hat{c}_{md}}{d\eta}\right|_{\eta=0} - V\hat{c}_{md}|_{\eta=0} = \left\{\frac{V}{2} - \sqrt{\frac{V^2}{4} + \frac{s}{Pe}}\right\}\hat{c}_{fd} + \delta(\xi)\exp\left[-\left(\frac{PeV}{2} + \sqrt{\left(\frac{PeV}{2}\right)^2 + sPe}\right)\eta_0\right] - V\hat{c}_{fd} \quad \text{(II-32)}$$

simplifying equation (II-32) gives,

$$\frac{1}{Pe}\frac{d\hat{c}_{md}}{d\eta}\bigg|_{\eta=0} - V\hat{c}_{md}\big|_{\eta=0} = -\left(\frac{V}{2}+\sqrt{\frac{V^2}{4}+\frac{s}{Pe}}\right)\hat{c}_{fd} + \delta(\xi)\exp\left[-\left\{\frac{PeV}{2}+\sqrt{\left(\frac{PeV}{2}\right)^2+sPe}\right\}\eta_0\right] \tag{II-33}$$

Substituting equation (II-33) into equation (II-28) gives,

$$\frac{d\hat{c}_{fd}}{d\xi}+\left\{s+\frac{V}{2}+\sqrt{\frac{V^2}{4}+\frac{s}{Pe}}\right\}\hat{c}_{fd} = \delta(\xi)\exp\left[-\left\{\frac{PeV}{2}+\sqrt{\left(\frac{PeV}{2}\right)^2+sPe}\right\}\eta_0\right] \tag{II-34}$$

Let

$$F(s) = s+\frac{V}{2}+\sqrt{\frac{V^2}{4}+\frac{s}{Pe}} \tag{II-35}$$

then Equation (II-34) becomes,

$$\frac{d\hat{c}_{fd}}{d\xi}+F\hat{c}_{fd} = \delta(\xi)\exp[(s-F)Pe\eta_0] \tag{II-36}$$

Integrating Equation (II-36) from $\xi=-\infty$ to ξ gives,

$$\hat{c}_{fd}(\xi,s) = H(\xi)e^{-F\xi}\exp[(s-F)Pe\eta_0] \tag{II-37}$$

where $H(\xi)$ is the step function:

$H(\xi)=0;\ \xi\le 0$

$H(\xi)=1;\ \xi>0$

Using Equation (II-35) for *F* in equation (II-37) gives,

$$\hat{c}_{fd}(\xi,s) = H(\xi)e^{-s\xi}\exp\left[-\left(\frac{V}{2}+\sqrt{\frac{V^2}{4}+\frac{s}{Pe}}\right)(\xi+Pe\eta_0)\right] \tag{II-38}$$

This is the result presented in Equation (88) of the main text.

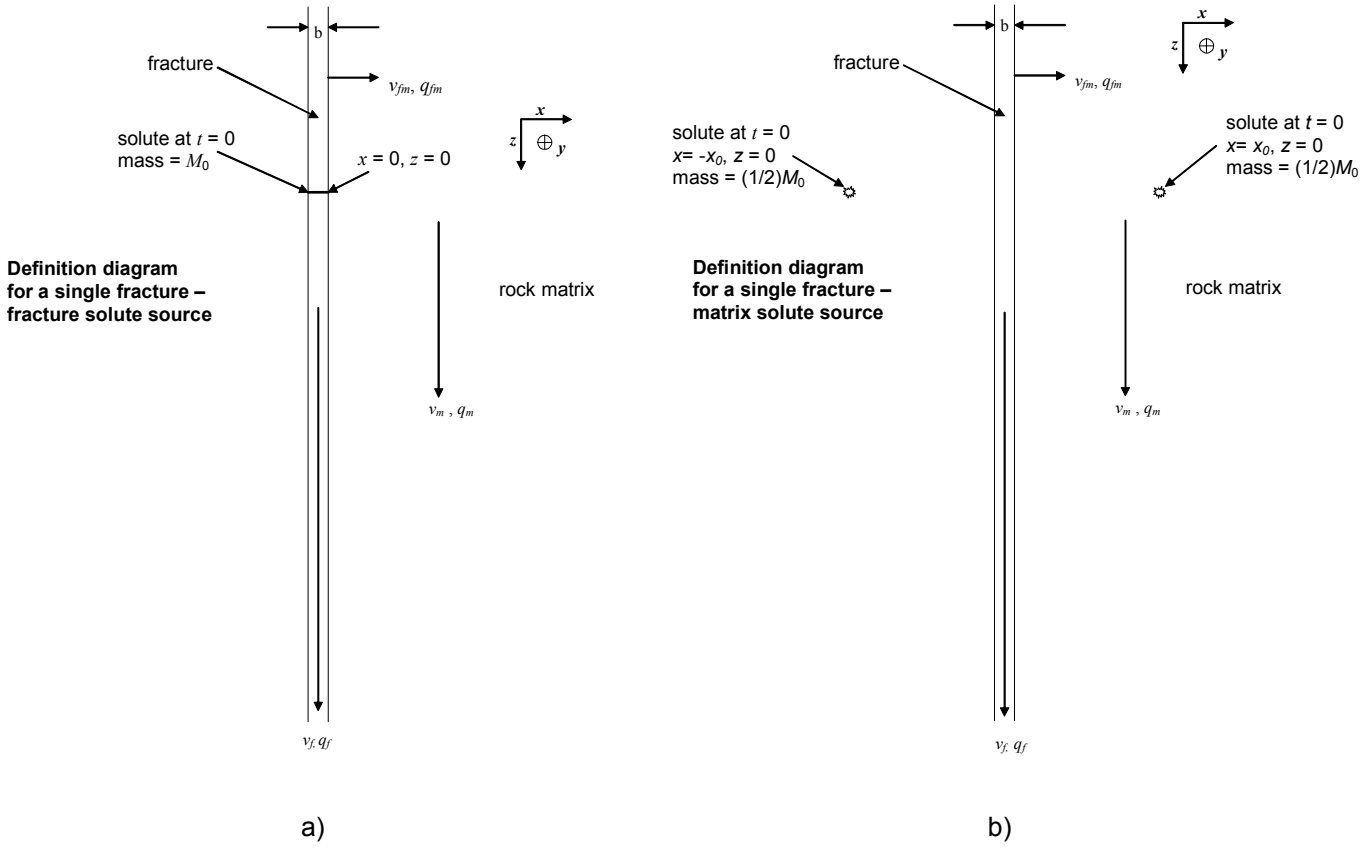

Figure 1. Definition diagrams for the single-fracture model. a) solute source in fracture; b) solute source in rock matrix.

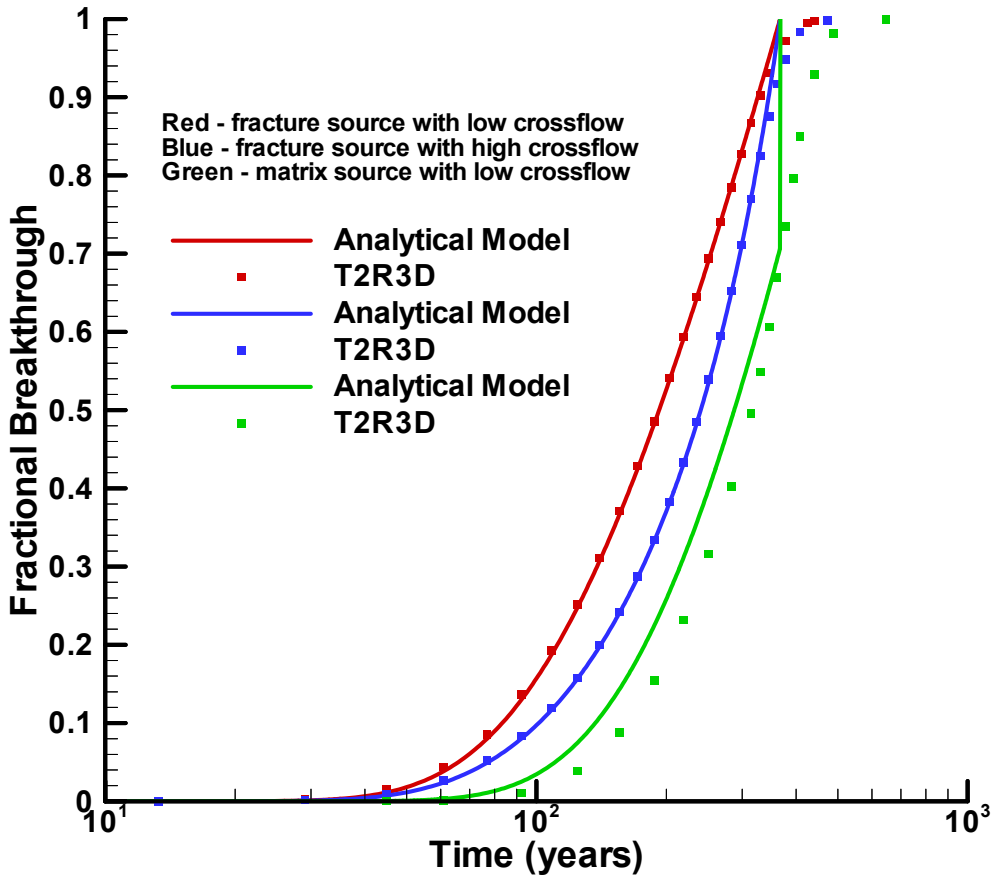

Figure 2. Breakthrough curves for an instantaneous point release and Peclet number of 37.

Note: Analytical model based on Equation (72) for fracture source and Equation (94) for matrix source. Peclet number for high cross-flow case is 38.

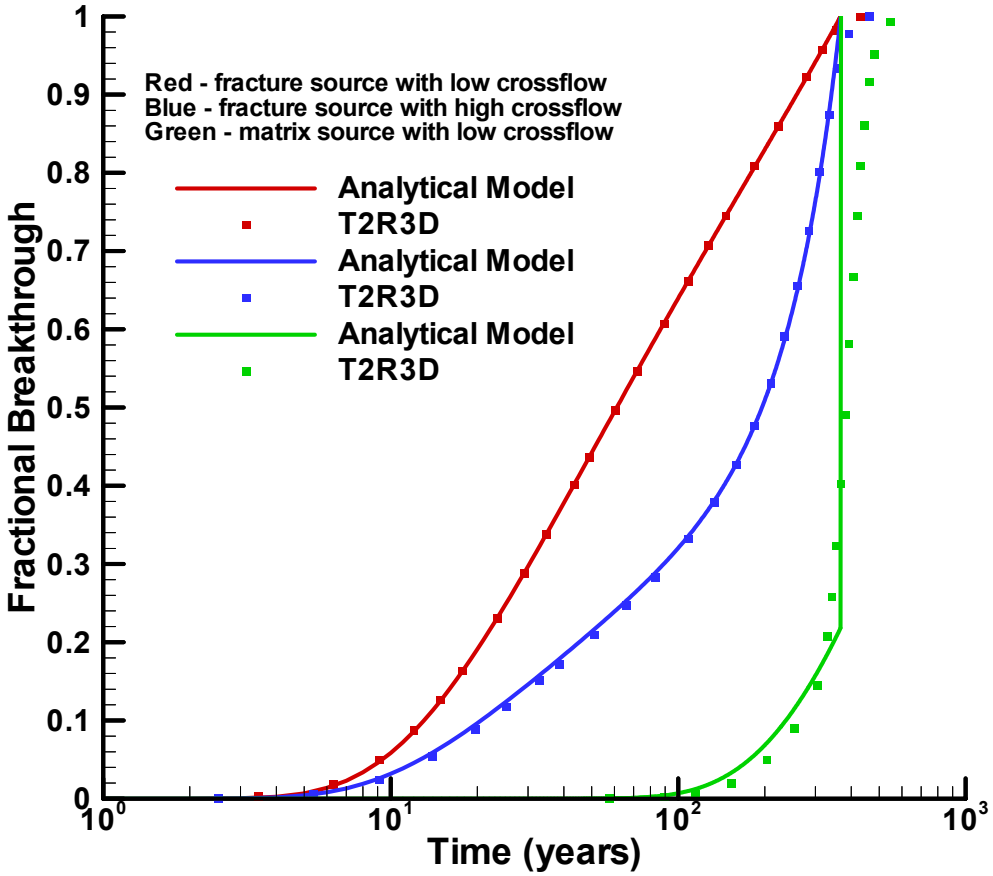

Figure 3. Breakthrough curves for an instantaneous point release and Peclet number of 370.

Note: Analytical model based on Equation (72) for fracture source and Equation (94) for matrix source. Peclet number for high cross-flow case is 380.

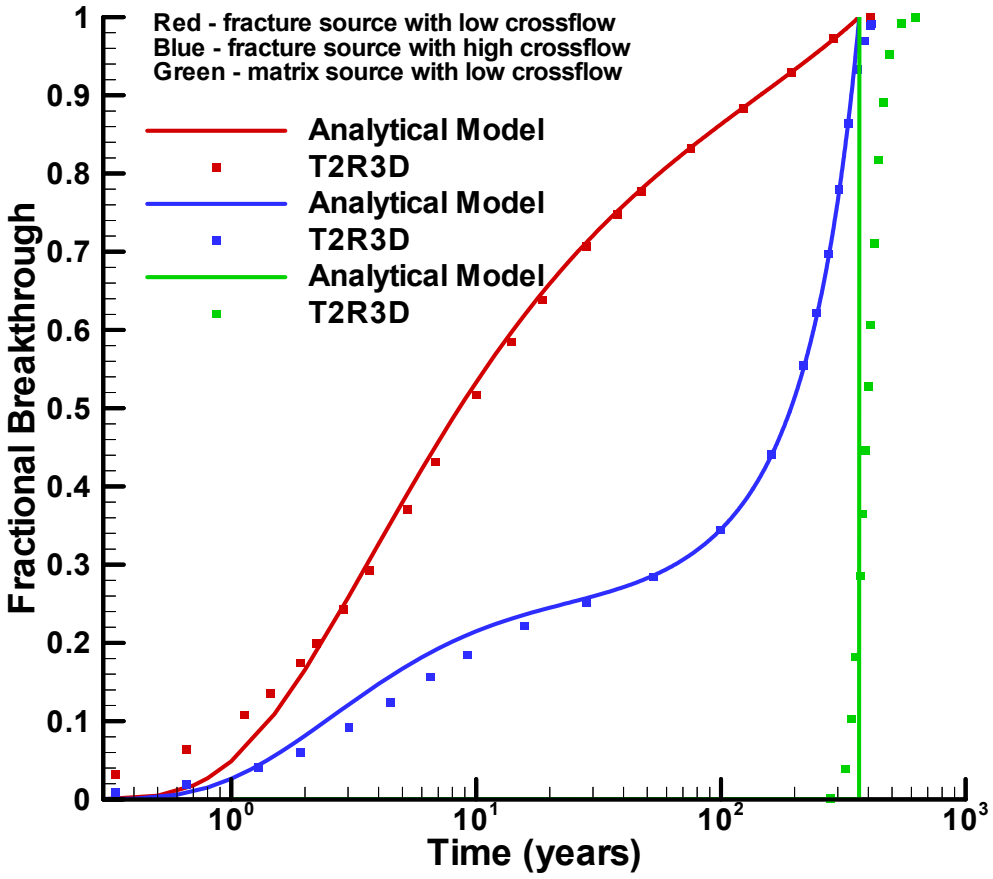

Figure 4. Breakthrough curves for an instantaneous point release and Peclet number of 3700.

Note: Analytical model based on Equation (72) for fracture source and Equation (94) for matrix source. Peclet number for high cross-flow case is 3800.

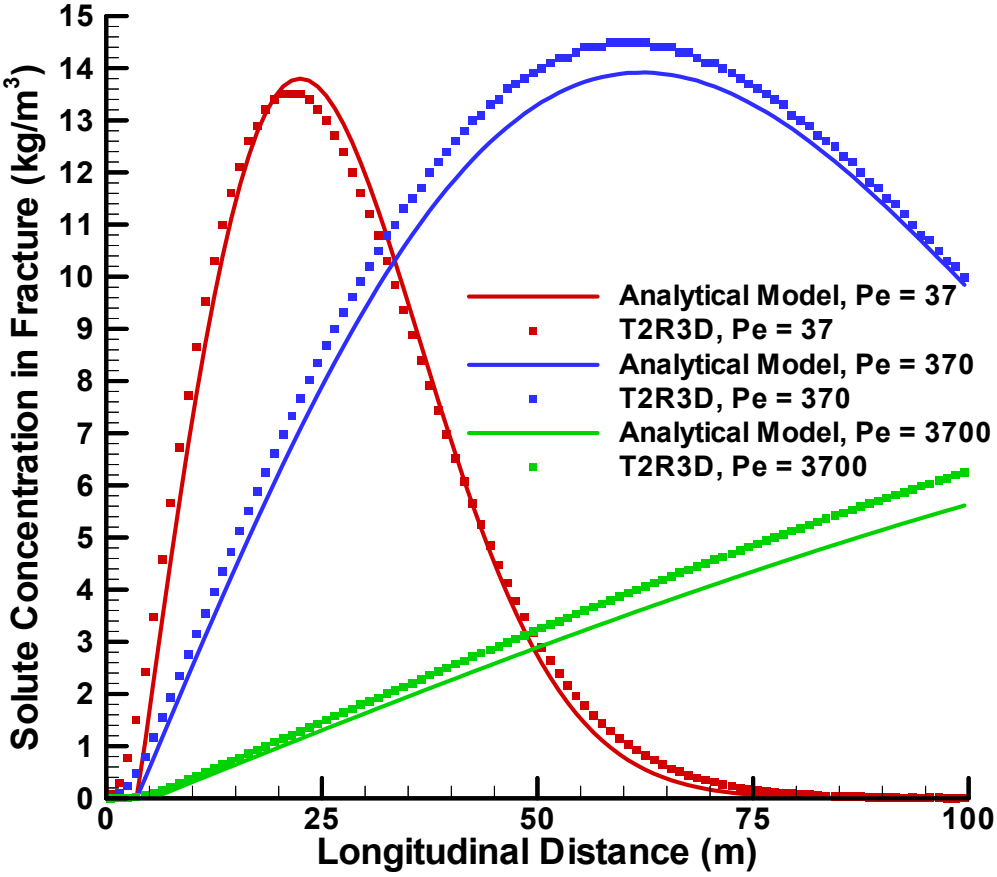

Figure 5. Concentrations profiles in the fracture from an instantaneous point release in the fracture at 13 years.

Note: Analytical model based on Equation (53). Low cross-flow case.

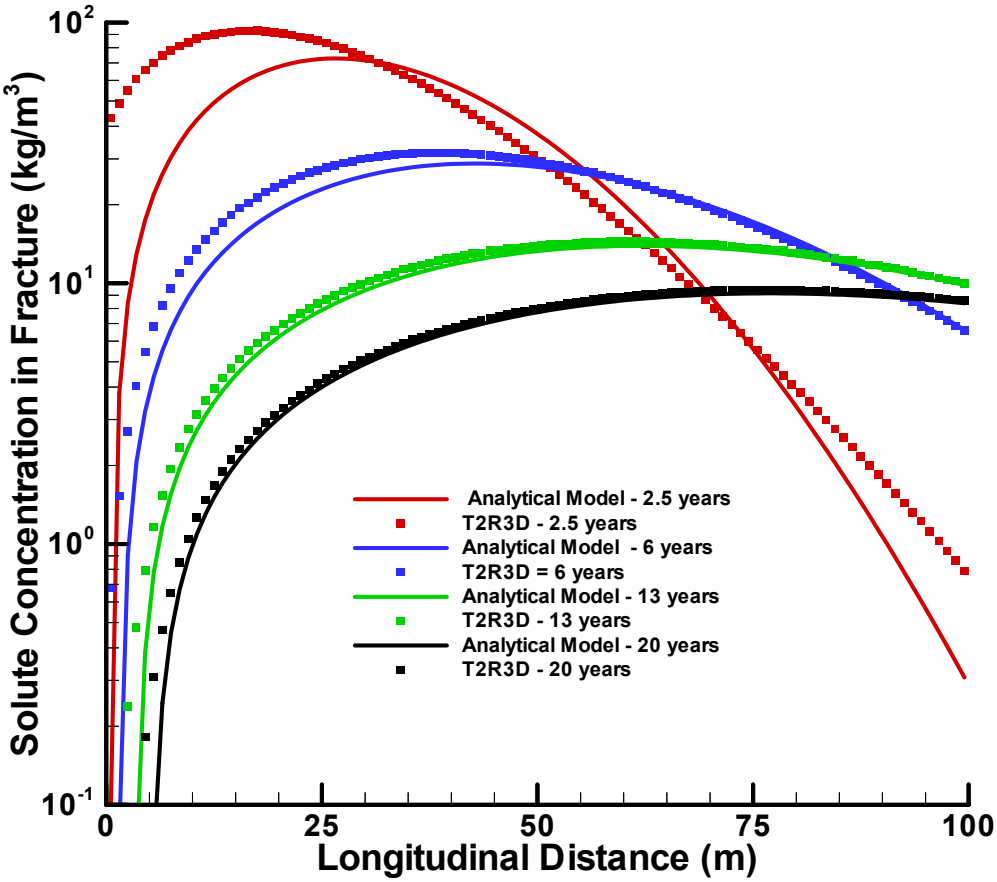

Figure 6. Concentrations profiles in the fracture from an instantaneous point release in the fracture for a Peclet number of 370.

Note: Analytical model based on Equation (55). Low cross-flow case.

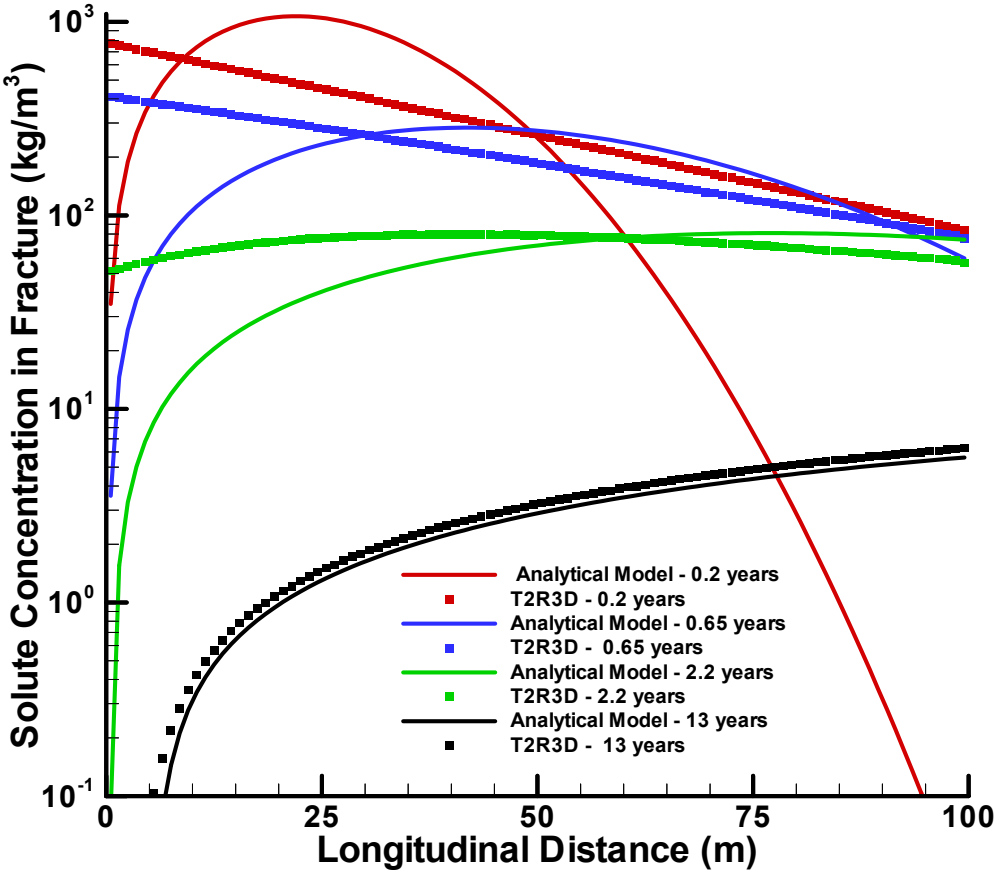

Figure 7. Concentrations profiles in the fracture from an instantaneous point release in the fracture for a Peclet number of 3700.

Note: Analytical model based on Equation (53). Low cross-flow case.

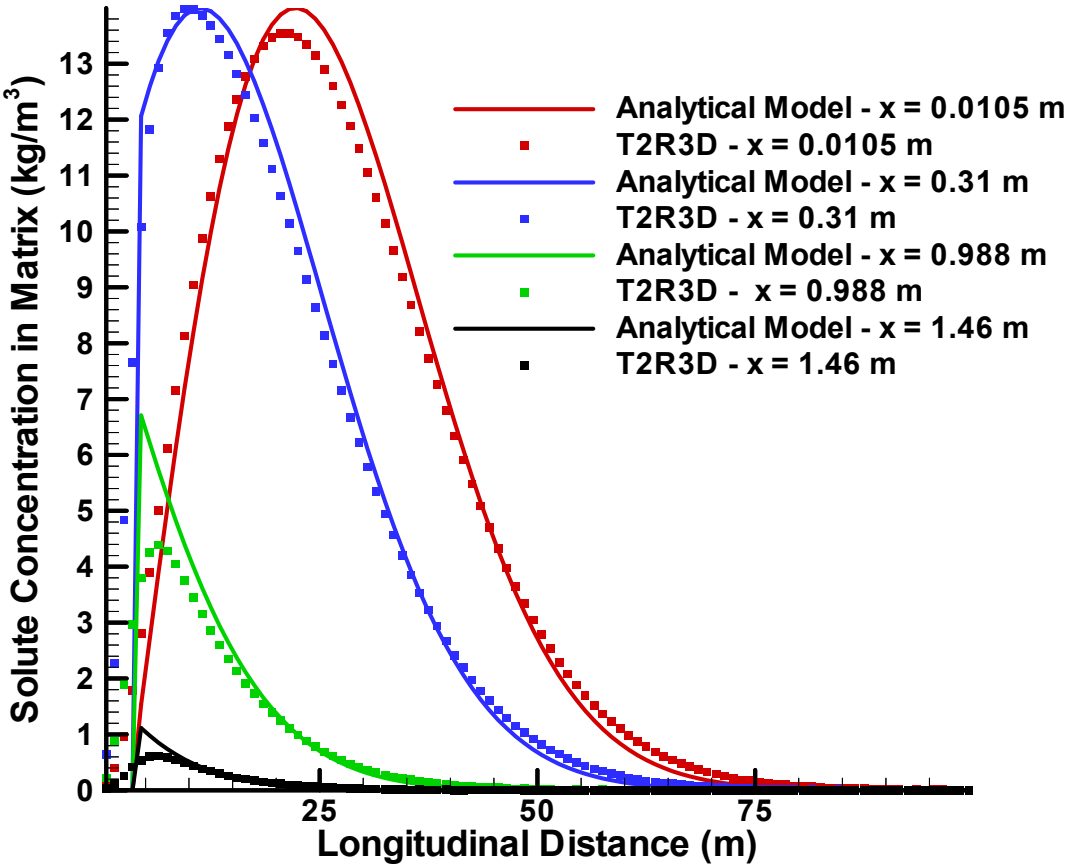

Figure 8. Concentrations profiles in the matrix from an instantaneous point release in the fracture for a Peclet number of 37.

Note: Analytical model based on Equation (56). The profiles are at 13 years after release of the solute. Low cross-flow case.

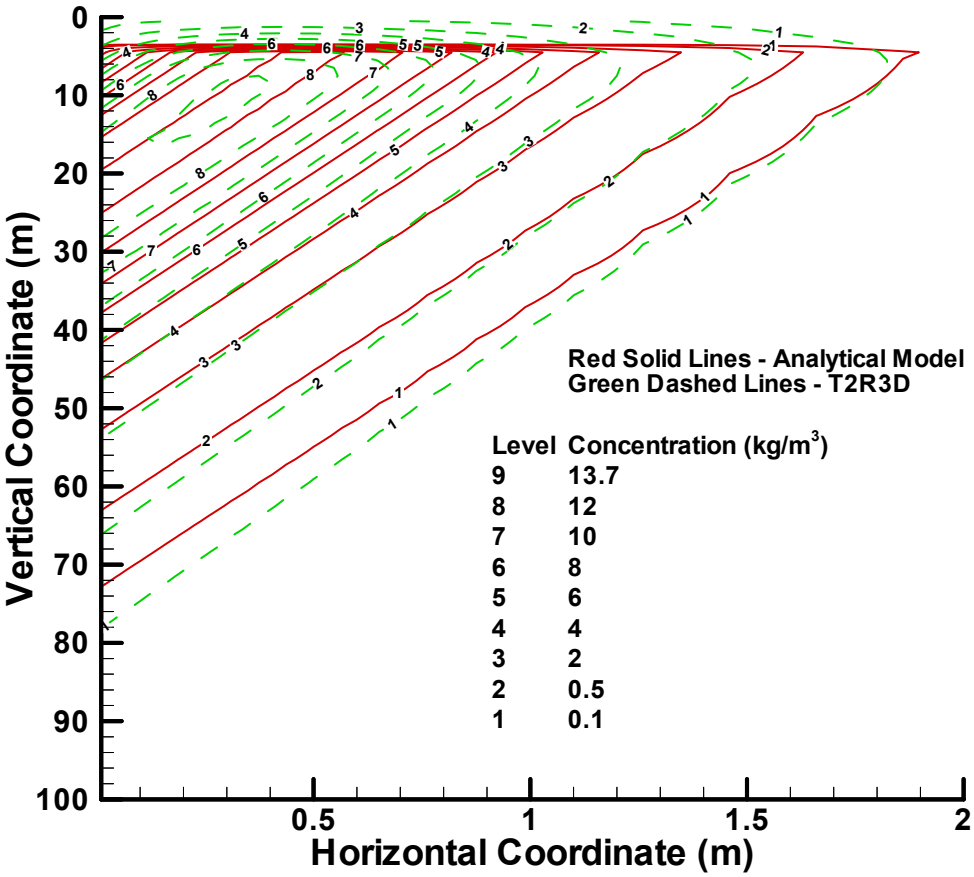

Figure 9. Solute concentration isopleths in the matrix from an instantaneous point release in the fracture for Peclet number = 37.

Note: Analytical model based on Equation (56). The isopleths are at 13 years after release of the solute. Low cross-flow case.

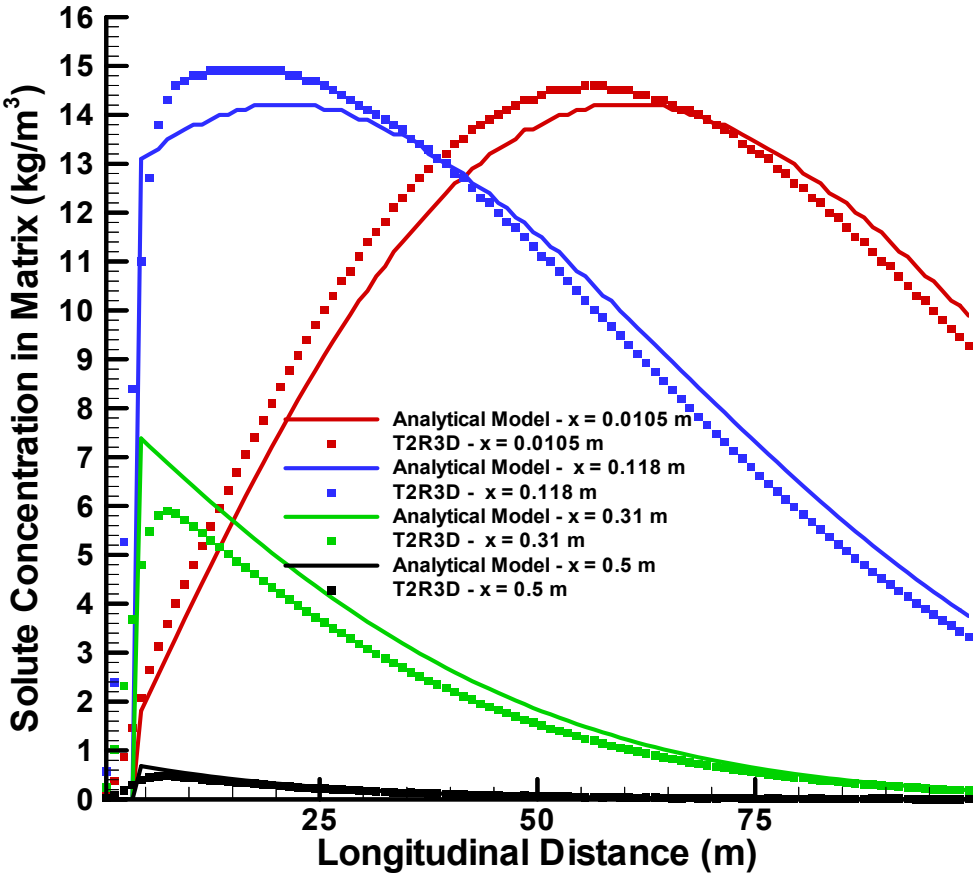

Figure 10. Concentrations profiles in the matrix from an instantaneous point release in the fracture for a Peclet number of 370.

Note: Analytical model based on Equation (56). The profiles are at 13 years after release of the solute. Low cross-flow case.

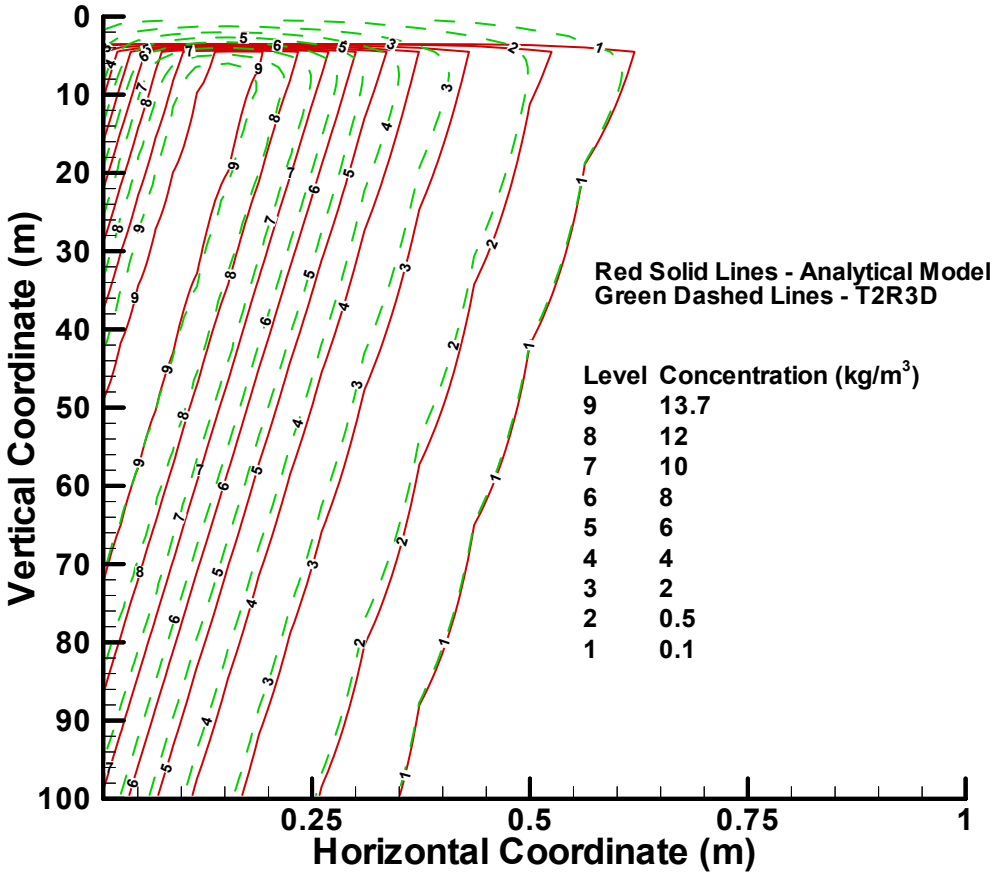

Figure 11. Solute concentration isopleths in the matrix from an instantaneous point release in the fracture for Peclet number = 370.

Note: Analytical model based on Equation (56). The isopleths are at 13 years after release of the solute. Low cross-flow case.

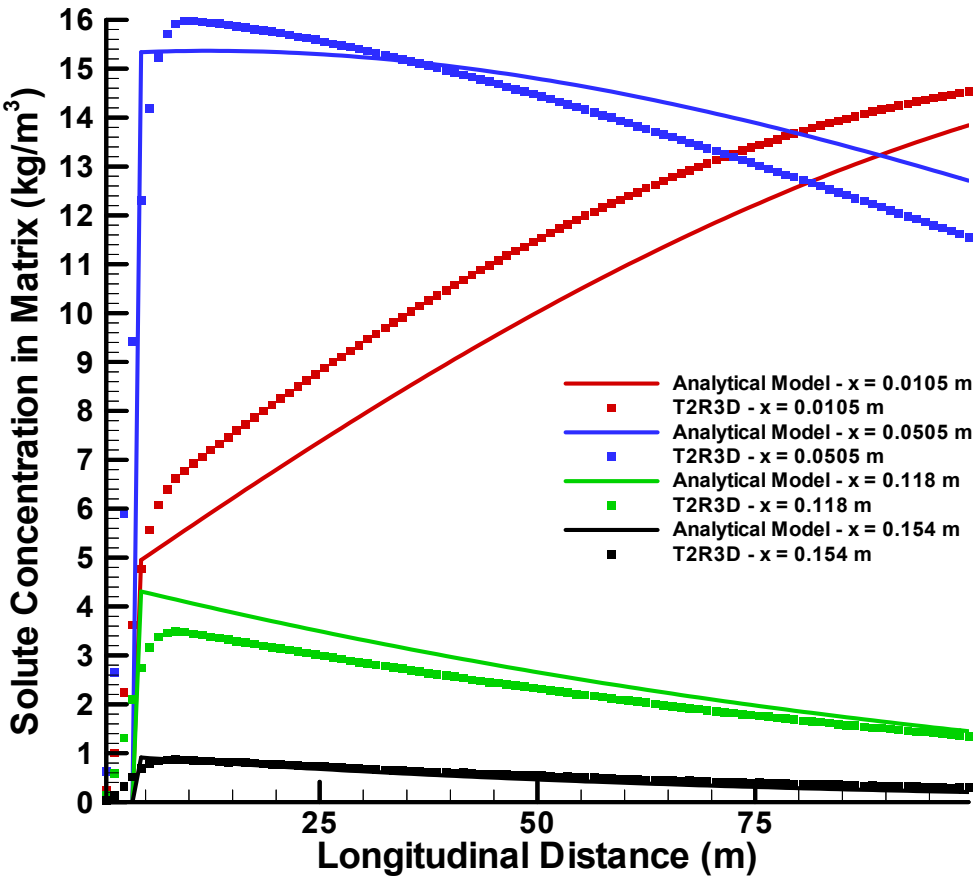

Figure 12. Concentrations profiles in the matrix from an instantaneous point release in the fracture for a Peclet number of 3700.

Note: Analytical model based on Equation (56). The profiles are at 13 years after release of the solute. Low cross-flow case.

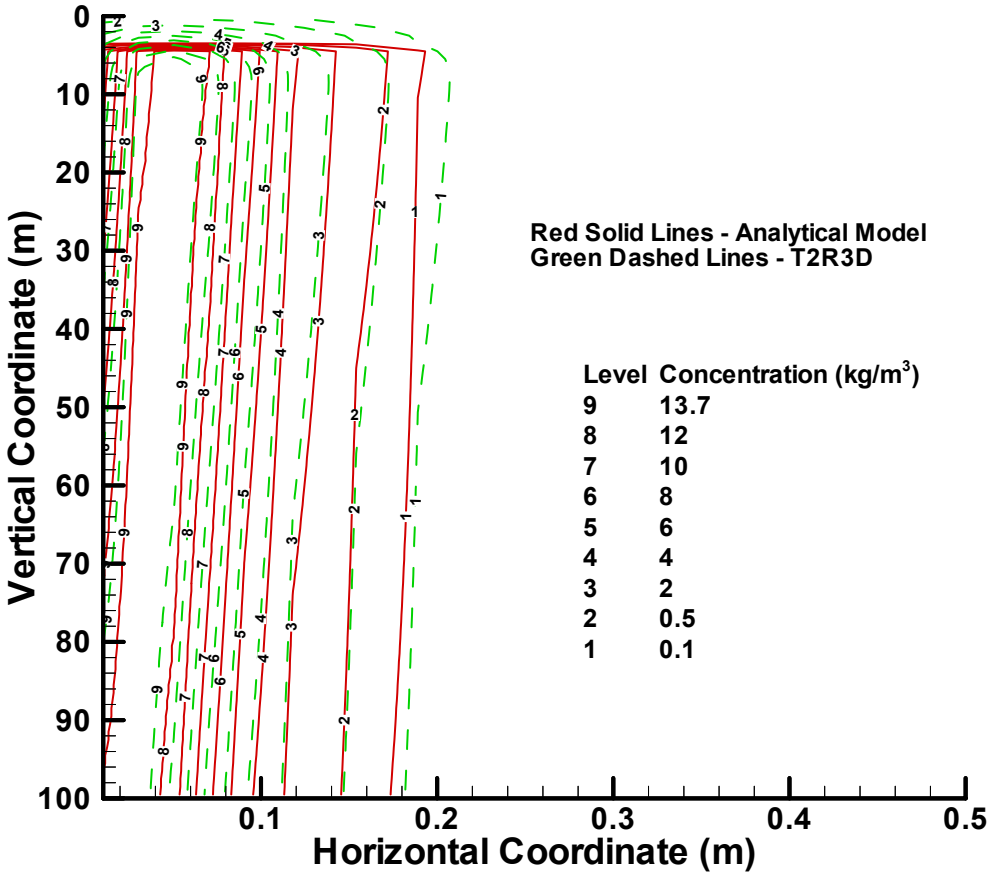

Figure 13. Solute concentration isopleths in the matrix from an instantaneous point release in the fracture for Peclet number = 3700.

Note: Analytical model based on Equation (56). The isopleths are at 13 years after release of the solute. Low cross-flow case.

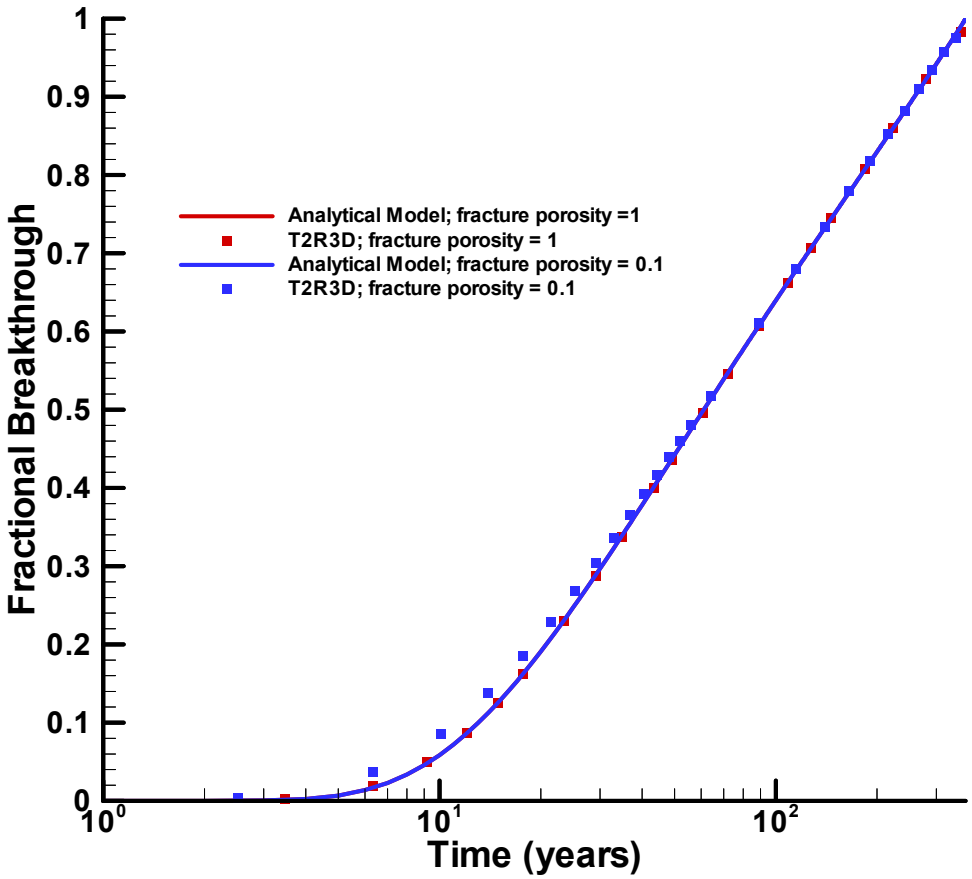

Figure 14. Breakthrough curves for an instantaneous point release in the fracture showing the effects of fracture porosity.

Note: Analytical model based on Equation (72). Low cross-flow case and Pe =370. Red line is not visible because it lies entirely beneath the blue line.

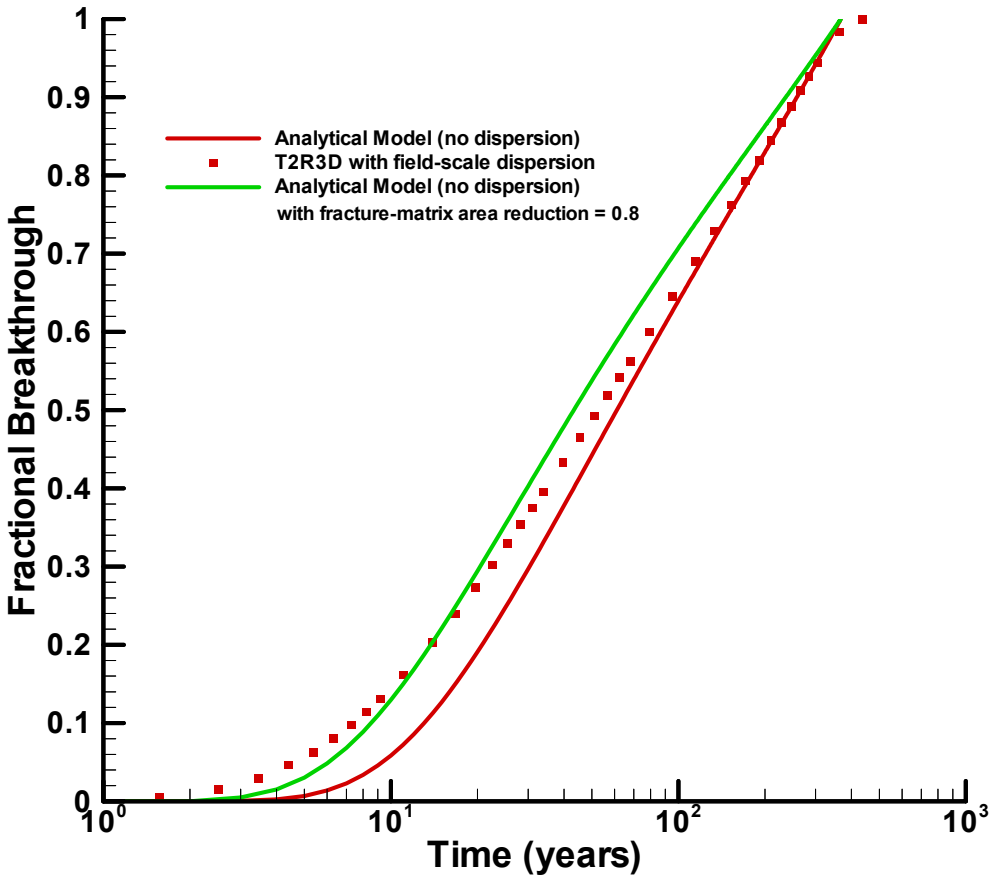

Figure 15. Breakthrough curves for an instantaneous point release in the fracture showing effects of longitudinal dispersion.

Note: Analytical model based on Equation (72). Fracture solute source with low cross-flow. Pe =370 for numerical (red points) and analytical model (red line). Pe = 460 for sensitivity case (green line), with reduced fracture-matrix interface area.